

AD-A245 761



NAVAL POSTGRADUATE SCHOOL Monterey, California

2



DTIC
SELECTE
FEB 11 1992
S B D

THESIS

EVALUATION OF COMPACT FELs
OPERATING AT 0.4 MICRON WAVELENGTH

by

Randy Souza
DECEMBER 1990

Thesis Advisor:

W.B. Colson

Approved for public release: Distribution is unlimited

92-02879



NCLASSIFIED

SECURITY CLASSIFICATION OF THIS PAGE

REPORT DOCUMENTATION PAGE

Form Approved
OMB No. 0704-0188

1 REPORT SECURITY CLASSIFICATION Unclassified		1b RESTRICTIVE MARKINGS	
2 SECURITY CLASSIFICATION AUTHORITY		3 DISTRIBUTION AVAILABILITY OF REPORT Approved for public release: Distribution is unlimited	
4 DECLASSIFICATION/DOWNGRADING SCHEDULE			
PERFORMING ORGANIZATION REPORT NUMBER(S)		5 MONITORING ORGANIZATION REPORT NUMBER(S)	
6a NAME OF PERFORMING ORGANIZATION Naval Postgraduate School	6b OFFICE SYMBOL (If applicable) PH	7a NAME OF MONITORING ORGANIZATION Naval Postgraduate School	
6c ADDRESS (City, State, and ZIP Code) Monterey, CA 93943-5000		7b ADDRESS (City, State, and ZIP Code) Monterey, CA 93943-5000	
8a NAME OF FUNDING/SPONSORING ORGANIZATION	8b OFFICE SYMBOL (If applicable)	9 PROCUREMENT INSTRUMENT IDENTIFICATION NUMBER	
6c ADDRESS (City, State, and ZIP Code)		10 SOURCE OF FUNDING NUMBERS	
		PROGRAM ELEMENT NO	TASK NO
		PROJECT NO	WORK UNIT ACCESSION NO
1 TITLE (Include Security Classification) EVALUATION OF COMPACT FELs OPERATING AT 0.4 MICRON WAVELENGTH			
2 PERSONAL AUTHOR(S) RANDY SOUZA			
3a TYPE OF REPORT Master's Thesis	13b TIME COVERED FROM _____ TO _____	14 DATE OF REPORT (Year, Month, Day) DECEMBER 1990	15 PAGE COUNT 83
6 SUPPLEMENTARY NOTATION The views expressed in this thesis are those of the author and do not reflect the official policy or position of the Department of Defense or the U.S. Government			
7 COSATI CODES		18 SUBJECT TERMS (Continue on reverse if necessary and identify by block number)	
FIELD	GROUP	SUB-GROUP	
		FEL, undulator, harmonics, oscillator, accelerator, gain	
9 ABSTRACT (Continue on reverse if necessary and identify by block number)			
<p>The behavior of Compact Free Electron Lasers is analyzed from a analytical and numerical point of view. The operating principles of the Compact FEL are reviewed with specific reference to electron dynamics, the gain mechanism, evolution of the optical field, and the generation of harmonics. Size and complexity of FEL systems can be substantially reduced by using micro-undulators that employ harmonics to reach optical wavelengths with low electron beam energy. The use of harmonics at short wavelengths improves the undulator design with longer periods that would be easier to fabricate. Numerical computer codes describing FEL physics are utilized to explore the advantages of using harmonics. Five methods that model various combinations of FEL physical effects with different levels of sophistication are used to obtain results of gain calculations. The plots show gain degradation due to energy spread and strong field saturation effects. An analysis of beam quality is used to arrive at new electron beam size limits that simplify gain analysis for all undulator designs.</p>			
20 DISTRIBUTION AVAILABILITY OF ABSTRACT <input checked="" type="checkbox"/> UNCLASSIFIED UNLIMITED <input type="checkbox"/> SAME AS RPT <input type="checkbox"/> DTIC USERS		21 ABSTRACT SECURITY CLASSIFICATION unclassified	
22a NAME OF RESPONSIBLE INDIVIDUAL W.B. Colson		22b TELEPHONE (Include Area Code) (408) 646-2765	22c OFFICE SYMBOL PH/Cw

D Form 1473, JUN 86

Previous editions are obsolete

SECURITY CLASSIFICATION OF THIS PAGE

S/N 0102-LF-014-6603

UNCLASSIFIED

Approved for public release: Distribution is unlimited

Evaluation of Compact FELs
Operating at 0.4 Micron Wavelength

by

Randy Souza
Lieutenant, United States Navy
B.S., Stonehill College, 1978

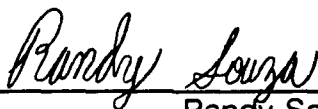
Submitted in partial fulfillment of the
requirements for the degree of

MASTERS OF SCIENCE
IN PHYSICS

from the

NAVAL POSTGRADUATE SCHOOL
DECEMBER 1990

Author:



Randy Souza

Approved by:



W.B. Colson, Thesis Advisor



Karlheinz E. Woehler, Second Reader



Karlheinz E. Woehler, Chairman
Department of Physics

ABSTRACT

The behavior of Compact Free Electron Lasers is analyzed from a analytical and numerical point of view. The operating principles of the Compact FEL are reviewed with specific reference to electron dynamics, the gain mechanism, evolution of the optical field, and the generation of harmonics. Size and complexity of FEL systems can be substantially reduced by using micro-undulators that employ harmonics to reach optical wavelengths with low electron beam energy. The use of harmonics at short wavelengths improves the undulator design with longer periods that would be easier to fabricate. Numerical computer codes describing FEL physics are utilized to explore the advantages of using harmonics. Five methods that model various combinations of FEL physical effects with different levels of sophistication are used to obtain results of gain calculations. The plots show gain degradation due to energy spread and strong field saturation effects. An analysis of beam quality is used to arrive at new electron beam size limits that simplify gain analysis for all undulator designs.



Accession For	
NTIS GRA&I	<input checked="checked" type="checkbox"/>
DTIC TAB	<input type="checkbox"/>
Unannounced	<input type="checkbox"/>
Justification	
By	
Distribution/	
Availability Codes	
Dist	Avail and/or Special
A-1	

TABLE OF CONTENTS

I.	INTRODUCTION	1
II.	BASIC PHYSICS OF THE FREE ELECTRON LASER	6
A.	DYNAMICS OF ELECTRON TRAJECTORIES	6
B.	GAIN MECHANISM FOR THE LOW-CURRENT, LOW-FIELD FEL	15
C.	DERIVATION OF THE OPTICAL WAVE EQUATION	19
D.	STRONG OPTICAL FIELDS AND SATURATION EFFECTS ...	28
E.	PRODUCTION OF HIGHER FREQUENCY HARMONICS IN FEL's	34
III.	CONCEPT OF A COMPACT FEL	40
A.	DEVELOPMENT OF THE PHOTO-CATHODE INJECTOR	41
B.	TECHNOLOGICAL ADVANCES IN MICRO- UNDULATOR DESIGNS	44
IV.	EVALUATION OF COMPACT FEL OPERATION	47
A.	HIGHER HARMONICS GENERATION IN COMPACT FELs .	47
B.	FEL SIMULATION METHODS	48
C.	COMPACT FEL DESIGN PARAMETERS	48

D.	GAIN DEGRADATION DUE TO BEAM QUALITY AND THE FILLING FACTOR	49
E.	METHODS OF ANALYSIS	55
1.	THREE-DIMENSIONAL SIMULATION CODES	55
a)	FELEX	55
b)	Wavefront simulation	57
2.	ONE-DIMENSIONAL SIMULATION CODE	58
3.	ANALYTICAL METHODS	58
a)	Integral equation	58
b)	Small-signal gain formula	58
F.	DISCUSSION OF PLOTS	61
V.	CONCLUSIONS	70
	LIST OF REFERENCES	71
	INITIAL DISTRIBUTION LIST	73

LIST OF FIGURES

Figure 1.	Schematic of the Interacting Elements of the FEL Oscillator	2
Figure 2.	Bunching Process of Electrons in the FEL	4
Figure 3.	Schematics for Perfect Electron Trajectories in Circular and Linearly Polarized Undulators	7
Figure 4.	Resonance Condition in the Free Electron Laser	13
Figure 5.	Weak-Field Gain Spectrum $G(\nu_0)$ For Moderate Current	20
Figure 6.	Differential Volume Element in the FEL	25
Figure 7.	Phase-Space Diagram For Weak Fields with Low Current	30
Figure 8.	Phase-Space Diagram For Weak Fields with Moderate Current	32
Figure 9.	Phase-Space Diagram For Strong Fields with Moderate Current	33
Figure 10.	The Gain Spectrum $G(\nu_0)$ for Moderate Current with Increasing Optical Field Strength a_0	34
Figure 11.	Schematic of Injection of Imperfect Electrons into Undulator	42
Figure 12.	Electron Particle Phase-Space Distribution	43
Figure 13.	Schematics of Compact FEL Operating on Optical and Undulator Harmonics	46

Figure 14.	Schematic for Diffraction of Light Wave in Undulator	54
Figure 15.	Gain Curve for Micro-undulator Design Operating on the Fundamental where Energy Spread is Varied	62
Figure 16.	Gain Curve for Micro-undulator Design Operating on the Fundamental where Optical Power is Varied	64
Figure 17.	Gain Curve for Micro-undulator Design Operating on the Third Harmonic where Energy Spread is Varied	65
Figure 18.	Gain Curve for Micro-undulator Design Operating on the Third Harmonic where Optical Power is Varied	66
Figure 19.	Gain Curve for Micro-undulator Design Operating on the Ninth Harmonic where Energy Spread is Varied	68
Figure 20.	Gain Curve for Micro-undulator Design Operating on the Ninth Harmonic where Optical Power is Varied	69

ACKNOWLEDGEMENTS

I wish to express my gratitude and appreciation to my advisor Professor William B. Colson for his instruction, guidance and endless hours of private conversation throughout this research. His expert knowledge in Free Electron Laser Theory is recognized throughout the world and having an opportunity to work with him provided a wave of excitement for this new and developing research area.

I wish to acknowledge the invaluable help of R. W. Warren, John C. Goldstein, and Richard L. Sheffield from the Free Electron Laser group at Los Alamos National Laboratory. They allowed me the opportunity to become involved in the Special Supporting Research Initiative Program Plan to Develop Advanced Free-Electron Laser Technology. This program provided involvement with technology of a new generation of FEL systems that would be available to a wider range of users.

Most importantly, my gratefulness to my loving wife, Caryn, for her devotion and patience that she continues to provide. Her sustained support furnished the catalyst for the pursuit of successfully completing my studies at the Naval Post Graduate School.

This work is dedicated to my father, Frank, for his strength and support he has given throughout my Naval career. I hope that his vitality will endure for many years to come.

I. INTRODUCTION

The free electron laser (FEL) is an adaptable source of coherent radiation that can operate at high power and has many potential applications in scientific research, industry, national defense and medicine. The FEL uses a high quality relativistic electron beam made to oscillate by passing through a periodic magnetic field to amplify coherent optical radiation [Ref. 1]. The basic FEL configuration (Figure 1) consists of an electron accelerator that injects a high-quality electron beam into the transverse periodic magnetic field called an "undulator." In the undulator, the interaction between the beam and the co-propagating radiation takes place. The electrons are the power source in the FEL, and can provide more than a gigawatt of peak power with an average power ranging from kilowatts to ten megawatts. The FEL converts the electron beam kinetic energy to electromagnetic radiation, and can be made to operate as an amplifier, or as an oscillator. In the first case, a high-current beam amplifies a low-power optical wave during a single pass through the interaction region without a need for a optical feedback system. In the second case, mirrors placed beyond each end of the undulator form a resonator, or optical cavity. In this cavity, radiation is reflected between the mirrors. Oscillating electrons are injected into the cavity to overlap the rebounding optical pulse. The laser field

grows on each pass, and becomes eventually large. In both cases, it is critical that the electrons spatially overlap the optical mode for energy exchange to occur between the electron beam and the electric field of the light wave [Refs. 2, 3].

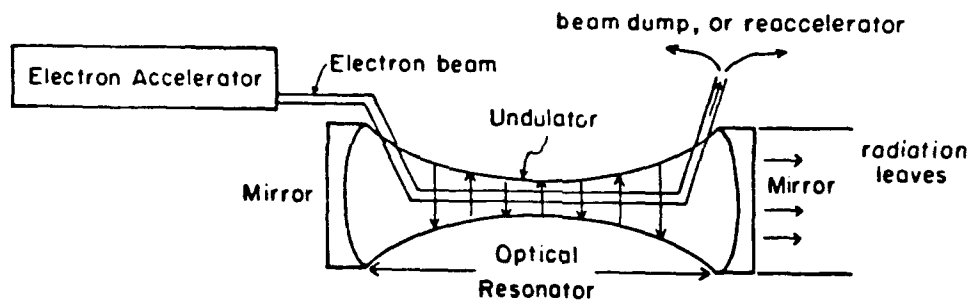


Figure 1. Schematic of the Interacting Elements of the FEL Oscillator. Successive electron pulses enter and propagate through the transverse periodic magnetic field set up by the undulator. The superimposed rebounding coherent optical wave is amplified by the electron beam energy exchange.

The basic physics of the FEL is analyzed theoretically by solving the relativistic electron particle dynamics, and coupling the solutions to Maxwell's optical wave equation [Ref. 4,5]. The three interacting elements of a high-quality relativistic electron beam, undulator-magnetic field that causes electrons to wiggle, and resonant optical cavity to provide feedback, combine to produce light at wavelengths that range from the microwave to the ultraviolet. The forward propagating electromagnetic wave and a transverse magnetic field, whose

electric and magnetic fields are perpendicular to the direction of propagation, give rise to an axial force that can extract energy from the electron beam.

The basic mechanism of the coherent energy exchange is the bunching of the electrons at optical wavelengths. The electrons leaving the accelerator are randomly positioned over many optical wavelengths. There are typically approximately 10^7 electrons, or more, in each section of the electron beam one optical wavelength of light long. As the light and electrons interact at the beginning of the undulator, some electrons gain energy and some lose energy. Those that gain energy move a little faster longitudinally and those that lose energy move a little slower; this eventually creates a bunch in each optical wavelength. See Figure 2. The bunching process, or localized spatial positioning of the electrons within a optical wavelength, is responsible for coherent radiation at the end of the undulator and creates the feedback process [Ref. 5].

As a consequence of the non-linear properties of the gain mechanism, higher harmonics of electromagnetic waves can be generated in FEL oscillators and amplifiers [Ref. 6,7]. The generation of harmonics in FELs can be used to reach optical wavelengths with moderate to low electron beam energy. This work discusses the advantages of using harmonics and contributes to the development of compact FELs where size and complexity can be substantially reduced. The compact FEL would use a micro-undulator with a length in the

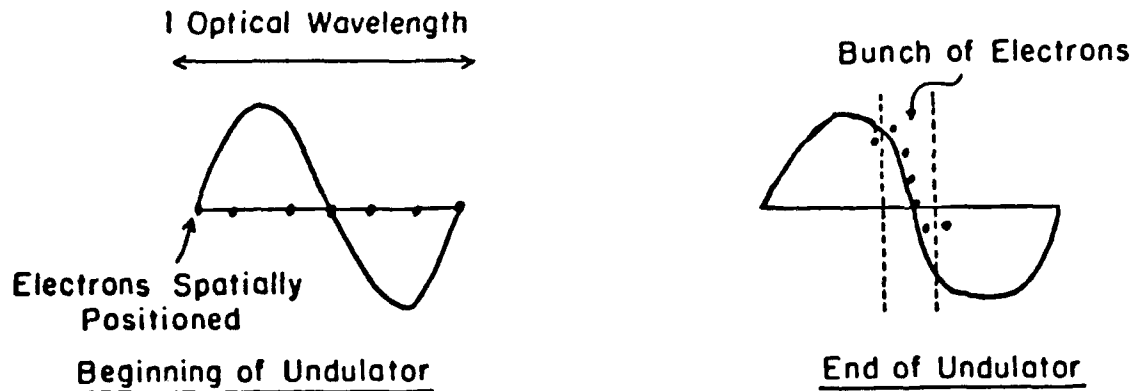


Figure 2. Bunching Process of Electrons in the FEL

Some of the electrons gain energy and some lose energy within one optical wavelength as they travel through the undulator. The electrons spatially overlap due to their different energies and cause amplification of light at the end of the undulator.

range of ten centimeters. The compact FEL would subsequently be made available to a much broader range of users [Ref. 8]. The considerable effort directed to the development of this device is motivated by the need to reach short wavelengths in the most inexpensive manner.

In Chapter II the development of the mathematics used to model the FEL interaction and describe the gain mechanism is outlined to provide the necessary background to understand the basic physics of the FEL. Chapter III discusses the concept of the compact FEL from the perspective of the accelerator and micro-undulator components of the FEL system and motivates the realization of these devices. The evaluation of three micro-undulators operating on harmonics at an optical wavelength of 0.4 microns are next explored in Chapter IV. An

analyses of the gain for these FEL systems and a careful discussion of the dependence on the electron beam quality is done in order to more fully understand the physics and define new limits on various parameters.

The author's most significant contributions made toward the operational advancement of a Compact Free Electron Laser are summarized below.

- Micro-undulator operation for proposed compact FEL devices are simulated to explore the wider use of harmonics in order to reach optical wavelengths with moderate-to-low electron beam energy.
- Gain degradation due to energy spread and strong field saturation effects are shown to demonstrate the advantages of using harmonics in order to reduce size and complexity of FEL systems.
- The Compact FEL designs are explored by five methods that model FEL physics with different levels of sophistication and mathematical formalism. The merits of predicating gain by each method are identified to establish their effectiveness to explore new designs.
- The data points on the curves in Figures 15 through 20 represent the result of several computer simulations that calculate the FEL gain using either a CRAY computer Sun Workstation, or Personal Computer.
- An analysis of beam quality is used to arrive at new electron beam size limits that simplify gain analysis for all undulator designs.

II. BASIC PHYSICS OF THE FREE ELECTRON LASER

A. DYNAMICS OF ELECTRON TRAJECTORIES

This section contains the derivation of the electron pendulum equation [Ref. 2-6], that calculates the dynamics of individual relativistic electrons as they are affected by the electric and magnetic fields in the laser cavity. The assumptions, approximations, and mathematical steps are presented in detail. Each electron's initial conditions determine the evolution of its velocity and position. This motion can be represented in periodic pendulum phase-space by a section of phase-space one optical wavelength long. The particular path each electron takes is determined by the amplitude of the undulator field and the optical fields. The physics can be understood by appealing to electron phase-space diagrams that consider the state of electron motion in the two-dimensional space of position and velocity. These diagrams will be utilized to study the FEL interaction and provide a method of evaluating the gain mechanism in the compact designs.

The electron evolution through an operating FEL's periodic undulator in cgs units, are governed by the Lorentz force equation:

$$\frac{d}{dt}(\gamma \vec{\beta}) = \frac{-e}{mc} \left[\vec{E}_r + \vec{\beta} \times (\vec{B}_u + \vec{B}_r) \right] \quad (1)$$

where e = magnitude of electron charge,
 m = mass of electron,
 c = speed of light,

$\vec{\beta}_c$ = electron velocity,
 \vec{B}_r = optical magnetic field,
 \vec{E}_r = optical electric field,
 \vec{B}_u = external magnetic field in undulator,
 γ = dimensionless Lorentz factor = $(1 - \vec{\beta} \cdot \vec{\beta})^{-1/2}$.

The undulator field seen by electrons can have circular polarization where the electron path in the laboratory frame of reference is helical along the z-axis. An alternative is an undulator with linear polarization where the electron path is sinusoidal in the x-z plane. See Figure 3.

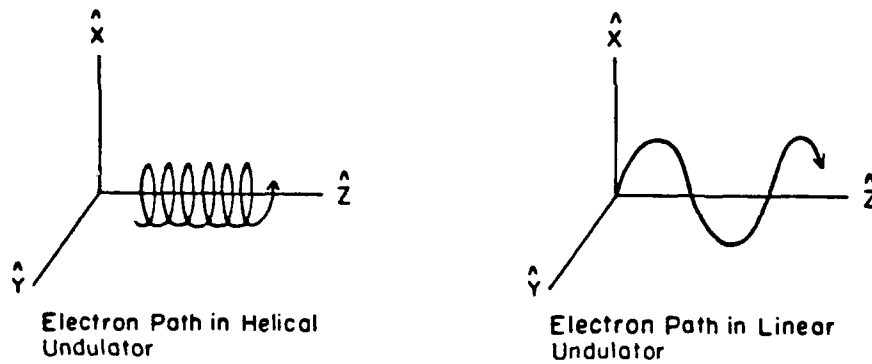


Figure 3. Schematics for Perfect Electron Trajectories in Circular and Linear Polarized Undulators.

The ideal helical undulator field near the z-axis in rectangular coordinates is

$$\vec{B}_u = [B_x, B_y, B_z] = B [\cos(k_o z), \sin(k_o z), 0] \quad (2)$$

where B = undulator peak magnetic field amplitude,
 k_o = undulator wave number = $2\pi/\lambda_o$,
 λ_o = undulator period,
 z = longitudinal position of electron along undulator.

It is important to realize that this representation of \vec{B}_u is accurate only near the z-axis, since away from the axis the transverse \vec{B}_u must bend to satisfy Maxwell's equation, $\vec{\nabla} \times \vec{B}_u = 0$.

The electric and magnetic fields of the radiation in the cavity are assumed to be a plane, circularly polarized, monochromatic wave. Both these fields travel along the z-axis with the electron. The fields are expressed in terms of the optical peak electric field amplitude and a sinusoidal disturbance:

$$\begin{aligned}\vec{E}_r &= E(t) [\cos\psi, -\sin\psi, 0] \\ \vec{B}_r &= E(t) [\sin\psi, \cos\psi, 0]\end{aligned}\tag{3}$$

where $E(t)$ = optical peak electric field amplitude,
 $\psi = kz - \omega t + \phi(t)$,
 k = optical wave number $= 2\pi/\lambda$,
 ω = carrier frequency $\omega = kc$,
 $\phi(t)$ = optical phase.

The simplest and most fundamental electromagnetic waves are transverse, plane waves where E and ϕ are independent of time and space z . The goal of the calculation is to determine how the details of the electron trajectories in the undulator are coupled to the light wave in the resonator cavity to produce a large optical power output.

The energy change for the relativistic electron in a radiation field is

$$\frac{d\gamma}{dt} = \frac{-e}{mc} (\vec{\beta} \cdot \vec{E}_r) \quad (4)$$

where $d(\gamma mc^2)/dt$ is the rate at which the electron loses or gains energy. An initial distribution of the electrons and velocities at the entrance of the undulator maybe chosen so that on the average the electron beam loses energy to the radiation field in one pass through a finite length of undulator. Figure 2, in the previous chapter, shows a distribution of electrons on the optical wavelength scale where an alteration of z-velocities provides coherent bunching at the end of the undulator to provide amplification of the radiation within the resonator.

The components of the Lorentz force equation and electron energy equation are

$$\begin{array}{c} \text{transverse component x-y plane} \\ \frac{d}{dt} (\gamma \vec{\beta}_\perp) = \frac{-e}{mc} [E (1 - \beta_z) (\cos\psi, -\sin\psi, 0) + \beta_z B (-\sin(k_o z), \cos(k_o z), 0)] \end{array} \quad (5a)$$

$$\begin{array}{c} \text{longitudinal component z-direction} \\ \frac{d}{dt} (\gamma \beta_z) = \frac{-e}{mc} [E (\beta_x \cos\psi - \beta_y \sin\psi) + B (\beta_x \sin(k_o z) - \beta_y \cos(k_o z))] \end{array} \quad (5b)$$

$$\dot{\gamma} = \frac{-e}{mc} E [\beta_x \cos\psi - \beta_y \sin\psi] \quad (6)$$

For relativistic electrons, $\beta_z \approx 1$, the electric and magnetic optical fields in (5a) nearly cancel. This implies $\beta_z B > E(1 - \beta_z)$ when $\beta_z \approx 1$. Therefore, the first term of the transverse component of the Lorentz force may be neglected for relativistic

electrons. The transverse electron velocity is determined almost entirely by the static magnetic field. This assumption allows the transverse component to be approximated by

$$\frac{d}{dt} (\gamma \beta_{\perp}) = \frac{-e}{mc} B (-\sin(k_0 z), \cos(k_0 z), 0). \quad (7)$$

Exact integration of this equation is allowed if we assume perfect injection of the electrons. This assumption removes the constants of integration and leads to the transverse velocity:

$$\beta_{\perp} = \frac{-K}{\gamma} (\cos(k_0 z), \sin(k_0 z), 0) \quad (8)$$

where K is the root-mean-square (rms) undulator parameter defined by

$$K = \frac{e \bar{B} \lambda_0}{2 \pi m c^2} \quad (9)$$

where $\bar{B} = B_{peak} / \sqrt{2}$ is the root-mean-square undulator magnetic field along the z -axis, and λ_0 is the undulator period. Perfectly injected electrons enter the undulator exactly on-axis without any random spread in angles or positions, i.e., $(x, y) = (0, 0)$, where x is the wiggle direction and y the direction of the magnetic field.

The undulator field gives the electron a small but important transverse "wiggle" velocity $\bar{\beta}_{\perp}$. The radiation fields alone have no significant effect on the electron's transverse trajectory, since forces due to E_r and B_r nearly cancel for relativistic electrons, $\gamma \gg 1$. Since total energy of the wave-particle must be

conserved, energy lost by the electron is gained by the light wave passing through the cavity according to (4). The relative orientation between $\vec{\beta}$ and \vec{E}_r is determined by the electron's initial position, z_0 within a radiation wavelength, λ . The determination of whether the electron gains or loses energy depends on the sign of $\dot{\gamma}$ in (4). When $\dot{\gamma}$ is positive, the electron gains energy and radiation is absorbed. When $\dot{\gamma}$ is negative, the electron loses energy as the radiation field grows, causing stimulated emission. The electron transverse velocity (8), and the electric field $\vec{E}_r = E (\cos\psi, -\sin\psi, 0)$ with a z-component can be used to solve the energy equation for $\gamma(t)$. Substituting into (4), the expressions for \vec{E}_r and $\vec{\beta}_\perp$ yields

$$\dot{\gamma} = \frac{-e}{mc} [E (\cos\psi, -\sin\psi, 0)] \cdot \left[\left(\frac{-K}{\gamma} \right) \cos(k_0 z), \sin(k_0 z), 0 \right].$$

Performing the vector dot product operation, and making use of the trigonometric identity $\cos(\psi + k_0 z) = \cos\psi \cos(k_0 z) - \sin\psi \sin(k_0 z)$ the above equation can be written as

$$\dot{\gamma} = \frac{eKE}{\gamma mc} \cos(\zeta + \varphi) \quad (10)$$

where $\zeta = (k + k_0) z - \omega t$ is the electron phase, and $k_0 z$ is the phase of the optical wave. Differentiating ζ with respect to z , for any $t > 0$, we see that $\Delta\zeta = (k + k_0) \Delta z$. For relativistic electrons $\beta_z \approx 1$, the optical wavelength λ is much smaller than the undulator period λ_0 , implying $k \gg k_0$. Therefore, $\Delta\zeta \approx k\Delta z$ describes the position of electrons on the optical wavelength scale with respect to

the combined optical and undulator forces. The actual electron beam initial conditions can be chosen so that the beam predominantly loses energy to the radiation field as the electrons travel through a finite length undulator. This gain mechanism will be discussed in the next section.

A more useful form of (10) can be obtained by relating the electron's energy to the electron's position in a section of the electron's beam one optical wavelength long. Equation (8) and the definition of the Lorentz factor in (1) can be equivalently written as $\gamma^{-2} = 1 - \beta_z^2 - \beta_\perp^2$ where $\beta_\perp^2 = K^2 / \gamma^2$. By eliminating $\beta_\perp^2 = K^2 / \gamma^2$ and solving for β_z^2 , we have

$$\beta_z^2 = 1 - \frac{1 + K^2}{\gamma^2}. \quad (11)$$

Taking the differential of β_z^2 with respect to time, $\dot{\gamma}$ is related to $\dot{\beta}_z$ by the following relationship

$$\frac{\dot{\gamma}}{\gamma} = \frac{\gamma^2}{1 + K^2} \beta_z \dot{\beta}_z. \quad (12)$$

In order to relate $\dot{\gamma}$ to $\ddot{\zeta}$, we must take the differential of $\zeta = (k + k_0)z - \omega t$, the electron phase velocity with respect to time, and solve for $\dot{\beta}_z$. The rate of change of the electron's velocity in the z-direction is given by $\dot{\beta}_z$. Substituting this result into (12), we see that

$$\frac{\dot{\gamma}}{\gamma} = \frac{\gamma^2}{1 + K^2} \beta_z \frac{\ddot{\zeta}}{(k + k_0)c}. \quad (13)$$

Recalling $k \gg k_0$ and $\beta_z \approx 1$, (13) can be written as

$$\frac{\dot{\gamma}}{\gamma} = \frac{\gamma^2}{(1 + K^2)} \frac{\dot{\zeta}}{\omega} \quad (14)$$

where $\omega = kc$.

At resonance, the electron has zero phase velocity $v=0$ and will pass through one undulator period as one optical wavelength passes over it. This resonance condition provides the maximum coupling and energy exchange between the electron's transverse velocity and the electric field but not necessarily the maximum transfer of power for the entire beam. See Figure 4.

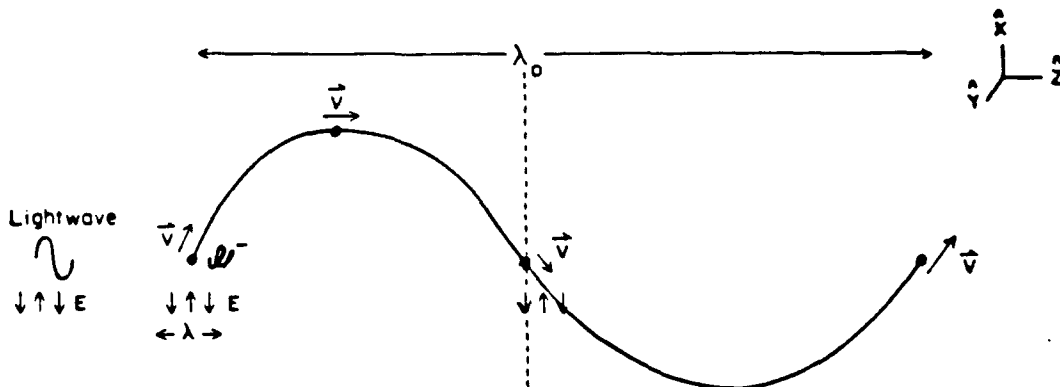


Figure 4. Resonance Condition in the Free Electron Laser.
In order for the work $\beta_{\perp} \cdot E$, to be positive the electron must move back an optical wavelength in transversing one undulator period.

For slow, efficient exchange to occur between the electron beam and the optical wave the electron phase ζ must remain close to 0, implying

$$(k + k_o) \beta_z c - \omega = 0 \text{ or}$$

$$k_o \beta_z = k (1 - \beta_z). \quad (15)$$

By making use of binomial expansion for $\gamma \gg 1$, (11) becomes

$$\beta_z = \left(1 - \frac{(1 + K^2)}{\gamma} \right)^{\frac{1}{2}} \approx 1 - \frac{1}{2} \left(\frac{1 + K^2}{\gamma^2} \right) \text{ or } (1 - \beta_z) = k \left(\frac{1 + K^2}{2\gamma^2} \right).$$

Substitution of this expression for $(1 - \beta_z)$ into (15) yields

$$k_o \beta_z = k \left(\frac{1 + K^2}{2\gamma^2} \right). \quad (16)$$

The resonance condition in terms of optical and undulator wavelengths for relativistic electrons, $\beta_z \approx 1$, is

$$\lambda = \lambda_o \left(\frac{1 + K^2}{2\gamma^2} \right). \quad (17)$$

Finally by making use of (10), (14), and the resonance condition, the non-linear pendulum equation describing electron particle dynamics in the FEL takes on the form:

$$\ddot{\zeta} = \frac{2eKE\omega_o}{\gamma^2 mc} \cos(\zeta + \varphi) \quad (18)$$

where $\omega_o = k_o c = 2\pi c / \lambda_o$.

The FEL interaction takes place while the light and electrons travel through the undulator. In the relativistic limit, the interaction time is close to L/c for both the light and the electron, where L is the length of the undulator. Define $\tau = ct/L$ as the dimensionless interaction time of the electron with the optical field as they

travel through the length of the undulator where $0 < \tau < 1$. The Pendulum equation takes the form:

$$\frac{d^2\zeta}{d\tau^2} = \left(\frac{4\pi NeKLE}{\gamma^2 mc^2} \right) \cos(\zeta + \varphi) \quad (19)$$

where N is the number of undulator periods.

Let

$$|a| = \left(\frac{4\pi NeKLE}{\gamma^2 mc^2} \right), \quad \ddot{\zeta} = \frac{d^2\zeta}{d\tau^2} \text{ and } v = \dot{\zeta} = \frac{d\zeta}{d\tau},$$

then the final equation becomes:

$\ddot{\zeta} = \frac{dv}{d\tau} = a \cos(\zeta + \varphi).$	<i>Pendulum Equation</i>
--	---------------------------------

The dimensionless optical field amplitude $|a|$ gives the strength of the coupling that occurs between ζ and v , and determines the electron bunching rate. For each electron traveling through the undulator, resonance is measured by the electron phase velocity v . The phase velocity is the difference between the frequency at which electrons pass over wavelengths of the undulator and frequency at which wavelengths of light pass over the electrons [Ref. 6]. The Pendulum equation describes the electron evolution where the initial electron's phase and phase velocity is defined by $\zeta(\tau=0) = \zeta_0$ and $v(\tau=0) = v_0$.

B. GAIN MECHANISM FOR THE LOW-CURRENT, LOW-FIELD FEL

A necessary attribute of the compact FEL is the ability to have a sufficient fractional increase in the optical power per pass through the undulator. This

requirement is important so that losses due to the low reflectivity and other optical resonator losses can be overcome [Ref. 9]. The laser oscillator is designed with mirrors carefully aligned so that light can bounce back and forth between these mirrors and have very little loss per bounce. A single pass of the electron beam is defined as the transport of the beam through the optical cavity from beginning to end of the undulator. If the net amplification between the mirrors, including scattering losses, exceeds the net reflection loss at the mirrors, the coherent optical power will build up in the system. A measure of the fractional increase in the optical power is called the gain G and defined by

$$G = \frac{\Delta P_{opt}}{P_{opt}}, \quad (20)$$

where ΔP_{opt} = change of power along the undulator
 P_{opt} = power at beginning of undulator.

The gain can also be expressed as the ratio of the energy lost by the electron beam to the power required to create the energy lost by the electron beam. It is assumed that the electrons do not interact with any other medium so that when the electron beam loses energy, all the energy is transferred to the light wave. This is critical in the start-up of the FEL where the strength of the optical field is initially very small. The following discussion highlights the derivation, assumptions and approximations of the low current-weak field gain formula [Ref. 4,5].

When the optical field is considered weak, $a \ll \pi$, there is little change in the electron phase velocity during the FEL interaction. On the first few passes of light in the oscillator, the optical field strength $|e|$, starts out very small. When the

dimensionless current is small, $j \ll 1$, there is little change in the optical field amplitude or phase in a single pass.

The assumptions used in this calculation of gain are:

- (1) the FEL is already operating and
- (2) the gain is low so that $\hat{a} \sim \text{small} \sim 0$.

Using the pendulum equation $\ddot{\zeta} = \dot{v} = |a| \cos(\zeta + \varphi)$, Ref. 5 solves for $v(\tau)$, the electron phase velocity, by using perturbation theory. This expression is given by

$$v(\tau) = v_o + \frac{a_o}{v_o} [\sin(\zeta_o + v_o \tau) - \sin(\zeta_o)] + \frac{a_o^2}{v_o^3} \left[-\frac{1}{4} (\cos(2\zeta_o + 2v_o \tau) - \cos(2\zeta_o)) + \cos(v_o \tau) - 1 - v_o \tau \sin(\zeta_o) \cos(\zeta_o + v_o \tau) \right] + \dots \quad (21)$$

where the initial optical field is $|a(o)| = a_o$ and $\varphi(o) = 0$.

The net change in energy of the electron beam is defined as "the energy electrons gain as work is done on them by the radiation field" minus "the energy electrons lose to the radiation field." A net change in energy of the electron beam does not occur for the term proportional to a_o because just as many electrons lose energy as gain energy. The higher-order terms proportional to a_o^2 in (21) will shift and skew the distribution of electron phase velocities so there can be a net change in the energy of the beam. To second order in a_o , there exists a net change in the electron energy given by

$$\langle v \rangle = v_o + \frac{a_o^2}{2v_o^3} [2 \cos(v_o \tau) - 2 + v_o \tau \sin(v_o \tau)]. \quad (22)$$

where $\langle \dots \rangle$ is used to denote a normalized average over the electrons.

The average energy lost by an electron is $\bar{\gamma} mc^2 (\langle v \rangle - v_o) / 4 \pi N$ [Ref. 5] where the electrons are assumed initially distributed uniformly in phase and mono-energetic with phase velocity v_o . The energy loss by all electrons ξ_e in the beam of volume element δV is therefore

$$\xi_e = \rho_e \delta V \frac{\bar{\gamma} mc^2 (\langle v \rangle - v_o)}{4 \pi N} \quad (23)$$

where ρ_e is the electron density. For low-gain the electrons are assumed to remain well inside the optical mode, and do not disturb the shape of the optical beam. The electron beam energy in volume element δV is deposited into the optical field during the FEL interaction. The radiation energy density that enters the optical field from the electron beam is governed by

$$\xi_{optical} = \frac{E^2 \delta V}{4 \pi} \quad (24)$$

where $\xi_{optical}$ = radiation energy density
 E = magnitude of circularly polarized radiation field
 δV = volume element of optical beam.

The gain is then found by taking the ratio of (23) and (24), and equating the energy loss by the electron beam to the energy gained by the light wave. The gain is

$$G = \frac{\Delta P_{opt}}{P_{opt}} = \frac{-\Delta \xi_e}{P_{opt}} = \frac{-\rho_e \bar{\gamma} mc^2}{E^2 N} \frac{a_o^2}{2 v_o^3} [2 \cos(v_o \tau) - 2 + v_o \tau \sin(\tau v_o)]. \quad (25)$$

Substituting (22) into the above expression, and defining a dimensionless current

$j = 8N(e\pi KL)^2 \rho_e / \gamma^3 mc^2$ the gain that occurs in the FEL is

$$G = j \frac{[2 - 2\cos(v_o \tau) - v_o \tau \sin(v_o \tau)]}{v_o^3} \quad (26)$$

This equation holds when gain is low. The gain spectrum is a plot of the final gain at $\tau=1$ versus the initial phase velocity v_o . The v_o -axis can be considered as a function of the optical wavelength centered at the resonant wavelength expressed by (17). The gain spectrum is anti-symmetric in v_o for $j \ll 1$ with a peak gain of

$$G = 0.135j \quad (27)$$

at $v_o=2.6$. At resonance, there is no gain, while at values of $v < 0$ there is net absorption of the optical power. A change in resonance of $\Delta v \approx \pi$ can shift the interaction from amplification to absorption. Shown in Figure 5 is the gain spectrum for moderate current, $j=5$, in weak optical fields $a_o=1$. The gain for this design is 80%. The gain spectrum is no longer anti-symmetric in v_o but shifted to the left where some gain at resonance now occurs. Since this dimensionless current corresponds to a moderate electron beam current, deviations of the spectrum from the low current case are expected.

Two corrections to (26) include (i) a coupling factor that incorporates Bessel functions that depend on K and the undulator polarization and (ii) a filling factor that includes the optical mode distortion effects [Ref. 5]. Both these factors are significant in FEL gain calculations and will be explored in Chapter IV.

C. DERIVATION OF THE OPTICAL WAVE EQUATION

We can derive a wave equation to describe the FEL's optical evolution. The assumptions, approximations and calculations found in [Ref. 2-6] are reviewed.

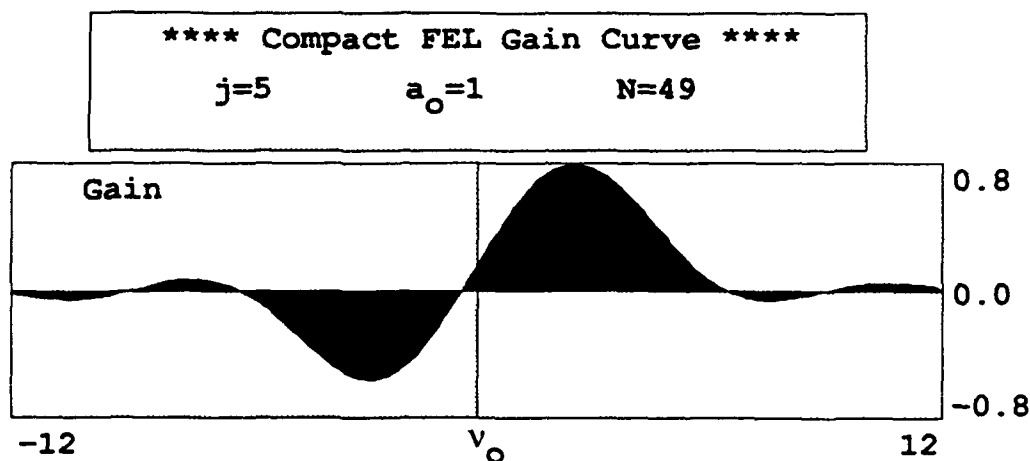


Figure 5. Weak-Field Gain Spectrum $G(v_j)$ For Moderate Current.

The purpose of the review is to provide the reader a basic understanding of the evolution of light in the presence of relativistic electrons that travel through a magnetic field set up by an undulator.

As relativistic electrons initially enter the undulator field, approximately one photon will be emitted for each electron that passes through the undulator. This is spontaneous emission. The total field from many electrons rapidly establishes a classical light wave. The number of electrons contained within the optical volume element δV depends on the electron density, and the ratio of the electron beam size to the optical mode size. As further amplification of the light wave occurs, approximately 10^6 photons per pass are emitted into the optical volume element causing the light to become a coherent emission source. This electromagnetic radiation provides the driving force on the oscillating electrons as they travel through the undulator. Using Maxwell's equations, the evolution of the amplitude and phase of the coherent optical wave can be coupled to the single-particle

Lorentz force equations. The electric field $E(z,t)$ changes in position and time due to the amplification process and the waveform passing over the electrons. The electric component of the optical field (3) can be approximately expressed by a radiation vector potential \vec{A} :

$$\vec{A} = \frac{E(t)}{k} (\sin\psi, \cos\psi, 0), \quad (28)$$

where $E(t)$ = electric field vector,
 $k = 2\pi/\lambda$,
 $\psi = kz - \omega t + \varphi(t)$ and $\varphi(t)$ = optical phase.

The amplitude of the electric field is assumed to be independent of the position z . It is also assumed that the electrons remain well inside the optical mode waist, and therefore, no transverse dimension considerations are included in the radiation vector potential.

By making use of the Lorentz gauge, the inhomogeneous wave equation [Ref. 10] becomes

$$\left[\nabla^2 - \frac{1}{c^2} \frac{\partial^2}{\partial t^2} \right] \vec{A} = \frac{-4\pi}{c} \vec{J}_\perp \quad (29)$$

where $\left[\nabla^2 - (1/c^2) \partial^2 / \partial t^2 \right]$ = wave operator,

$$\nabla^2 = (\partial^2 / \partial x^2, \partial^2 / \partial y^2, \partial^2 / \partial z^2)$$

\vec{J}_\perp = transverse electron current density source term.

This expression describes a plane wave traveling in the z -direction when the amplitude and phase are held fix. When the amplitude and phase slowly evolve over an optical wavelength, first and second derivatives in the spatial and time domains, and terms containing two derivatives can be neglected, since the

radiation bandwidth is emitted in a narrow spectrum. Substituting (28) into (29) and using this approximation, the left side of the wave equation can be simplified to [Ref. 5]

$$\left[\nabla^2 - \frac{1}{c^2} \frac{\partial^2}{\partial t^2} \right] \vec{A}(t) = \frac{2}{c} \frac{\partial E}{\partial t} (\cos \psi, -\sin \psi, 0) - \frac{2E}{c} \frac{\partial \phi}{\partial t} (\sin \psi, \cos \psi, 0). \quad (30)$$

Equations that are slowly-varying can be constructed by projecting the wave equation on two unit vectors in the following manner:

$$\left[\nabla^2 - \frac{1}{c^2} \frac{\partial^2}{\partial t^2} \right] \vec{A}(t) \cdot \hat{e}_1 = \frac{-4\pi}{c} \vec{J}_\perp(t) \cdot \hat{e}_1 \quad (31)$$

$$\left[\nabla^2 - \frac{1}{c^2} \frac{\partial^2}{\partial t^2} \right] \vec{A}(t) \cdot \hat{e}_2 = \frac{-4\pi}{c} \vec{J}_\perp(t) \cdot \hat{e}_2 \quad (32)$$

where

$$\hat{e}_1 = (\cos \psi, -\sin \psi, 0) \quad (33a)$$

$$\hat{e}_2 = (\sin \psi, \cos \psi, 0). \quad (33b)$$

The fast factors "cos (ψ)" and "sin (ψ)" each oscillate once as an electron near resonance passes through an undulator period.

The substitution of (30) for $\left[\nabla^2 - (1/c^2) \partial^2 / \partial t^2 \right] \vec{A}(t)$ and (33a) for \hat{e}_1 are made into the left side of (31). A similar procedure is performed with (33b) for \hat{e}_2 and the left side of (32). Performing the vector dot product operation on the left side, Maxwell's equations become:

$$\frac{1}{c} \frac{\partial E}{\partial t} = \frac{-2\pi}{c} \bar{J}_{\perp}(t) \cdot \hat{e}_1 \quad (34)$$

$$\frac{E}{c} \frac{\partial \phi}{\partial t} = \frac{2\pi}{c} \bar{J}_{\perp}(t) \cdot \hat{e}_2. \quad (35)$$

The source term $\bar{J}_{\perp}(t)$ describes the electron current density as a function of the time the electrons interact with the optical wave and the longitudinal position of the electron in the undulator. The single particle current density is determined by [Ref. 10]:

$$\bar{J}_{\perp i} = -ec \bar{\beta}_{\perp} \delta^{(3)}(\vec{x} - \vec{r}_i) \quad (36)$$

where $\bar{J}_{\perp i}$ = transverse electron current density source term of the i th electron
 e = charge of electron
 c = speed of light
 $\bar{\beta}_{\perp}$ = transverse electron velocity
 $\delta^{(3)}(\vec{x} - \vec{r}_i)$ = delta-function that describes the electron's location at position \vec{x} in 3-dimensional space
 \vec{r}_i = trajectory of the i th electron.

Since Maxwell's equations are driven by the total beam current, the sum of all the electrons particle currents must be determined. Equation (36) is modified accordingly:

$$\bar{J}_{\perp} = \sum_i \bar{J}_{\perp i} = -ec \sum_i \bar{\beta}_{\perp} \delta^{(3)}(\vec{x} - \vec{r}_i) \quad (37)$$

where the sum is over all i electrons located in a small volume element δV .

The electron's transverse motion is almost entirely determined by the undulator field, so (8) can accurately be used to express in the total beam current.

Using (8), (36), (33a) and (33b), the right side of Maxwell's first-order scalar equation, (34), is transformed into

$$\frac{-2\pi}{c} \vec{J}_\perp(t) \cdot \hat{e}_1 = \frac{-2\pi eK}{\gamma} \sum_i \delta^{(3)}(\vec{x} - \vec{r}_i) [\cos(k_o z) \cos\psi - \sin(k_o z) \sin\psi].$$

Using the trigonometric identity $\cos(k_o z + \psi) = \cos(k_o z) \cos\psi - \sin(k_o z) \sin\psi$, the final form of the transverse electron current density projected along \hat{e}_1 is

$$\vec{J}_\perp(t) \cdot \hat{e}_1 = \frac{ceK}{\gamma} \sum_i \delta^{(3)}(\vec{x} - \vec{r}_i) \cos(k_o z + \psi). \quad (38)$$

Following similar manipulations with (8), the final form of the transverse electron current density projected along \hat{e}_2 is

$$\vec{J}_\perp(t) \cdot \hat{e}_2 = \frac{ceK}{\gamma} \sum_i \delta^{(3)}(\vec{x} - \vec{r}_i) \sin(k_o z + \psi). \quad (39)$$

Substituting the electron current density equations (38) and (39) into Maxwell's two first-order scalar equations, (34) and (35), we acquire:

$$\frac{1}{c} \frac{\partial E}{\partial t} = \frac{2\pi eK}{\gamma} \sum_i \delta^{(3)}(\vec{x} - \vec{r}_i) \cos(k_o z + \psi) \quad (40)$$

$$\frac{E}{c} \frac{\partial \phi}{\partial t} = \frac{-2\pi eK}{\gamma} \sum_i \delta^{(3)}(\vec{x} - \vec{r}_i) \sin(k_o z + \psi). \quad (41)$$

In order to proceed further, the volume element where the FEL interaction occurs must be defined. This differential volume, δV , determines how the appropriate approximations of the electric field's slowly-varying time and space coordinates are made, and also provides a means to sample all the electrons that are contained in this space. The electron and optical beams are both considered cylindrical

where natural diffraction of the light is ignored, and electrons are well inside the optical mode waist. See Figure 6.

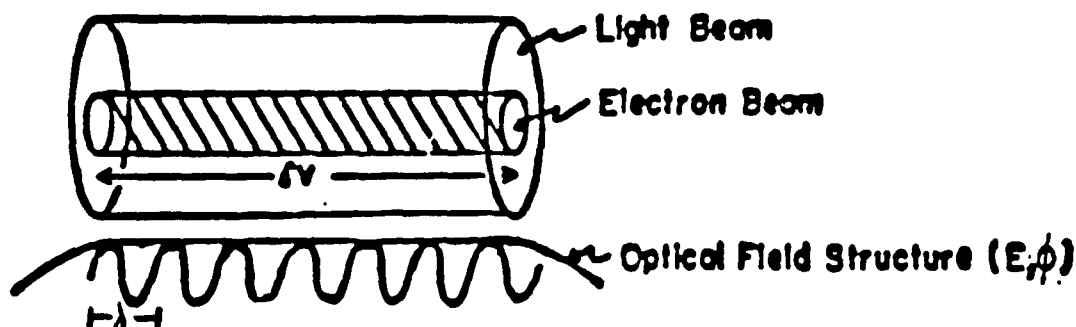


Figure 6. Differential Volume Element in the FEL

Simplification to the light and electron beams are made so the electron beam remains well inside the optical beam where both are taken to be cylindrical in shape. Also, shown are several optical wavelengths inside the optical field contained in δV .

The volume element is chosen so that it contains several wavelengths of light in which the optical field structure (E, ϕ) remains essentially constant. An averaging process of (40) over this volume element for the optical field amplitude and electron particle positions must be performed to remove δ -functions. By averaging over an element δV that is much smaller than the size of the optical field envelope, all the field sites will have essentially the same slopes and time derivatives. This results in the left side of (40) remaining unchanged. The right side also must be averaged over many optical wavelengths where all the δ -functions that exist within the volume element δV must be summed. Since the average is over many optical wavelengths, a large number of electrons are either bunched or randomly positioned. The electron phase ζ will provide a means of locating electrons within 0 to 2π in phase space. The function $\cos(k_z z + \psi(0)) = \cos[(k_0 + k)z]$ at $t=0$ and

$\varphi(z,t)=0$ can be approximated as $\cos(kz_0)$ for $k \gg k_0$. Recalling, for any $t>0$ and $k \gg k_0$, ψ follows the electron position in a section of the beam one optical wavelength long, $\Delta\zeta \approx k\Delta z$. Therefore, the position of the electron within an optical wavelength is simply given by $\zeta = kz$.

The sum $\sum_i \delta^{(3)}(\vec{x} - \vec{r}_i) \cos(k_0 z + \psi)$ electrons in δV can be replaced by an average over sampled electrons within the optical wavelength $\sum_i \delta^{(3)}(\vec{x} - \vec{r}_i) \langle \cos(\zeta + \phi) \rangle$ where $k_0 z + \psi = \zeta + \phi$ and $\langle \cos(\zeta + \phi) \rangle$ is the averaged sum. The sum of the δ -functions for all electrons in the volume element δV can be converted to an electron particle density, ρ_e , that will properly weight the average sum of the sampled electrons $\langle \cos(\zeta + \phi) \rangle$ and correctly determine how much the optical wave is driven by all electrons in δV . The form of the field envelope is assumed to depend on both z and t . Combining these assumptions and approximations (40) can be written as

$$\frac{dE}{dt} = \frac{2\pi c e K}{\gamma} \rho_e \langle \cos(\zeta + \phi) \rangle. \quad (42a)$$

The evolution of the optical phase is determined by performing a similar weighted average over sample electrons in the microscopic volume element:

$$\sum_i \zeta^{(3)}(\vec{x} - \vec{r}_i) \sin(k_0 z + \psi) = \rho_e \langle \sin(\zeta + \phi) \rangle$$

where now (41) is written as

$$E \frac{d\phi}{dt} = \frac{-2\pi c e K}{\gamma} \rho_e \langle \sin(\zeta + \phi) \rangle. \quad (42b)$$

These two non-linear equations are coupled through the electron pendulum equation, and describe the long-term evolution of the amplitude and phase of the laser field. Using the dimensionless parameters

$$|a| = \frac{4\pi N e K L E}{\gamma^2 m c^2}, \quad \tau = \frac{c t}{L} \quad j = 8N (e \pi K L)^2 \frac{\rho_e}{\gamma^3 m c^2} \quad \text{and}$$

defining $a = |a| e^{i\phi}$, (42a) is put in complex form:

$$\dot{a} = \frac{da}{d\tau} = -j \langle e^{-i\zeta} \rangle.$$

Optical Wave Equation

The utility of this equation in expressing gain can be immediately seen by considering values of ζ that either maximize or minimize the real part of $\langle e^{-i\zeta} \rangle$. Examining this equation, we can see that bunching of the beam at $\zeta = \pi$ will drive the amplitude of the optical wave, and lead to gain. Growth of the wave also occurs with increased dimensionless current j and depends on the electron distribution $\langle \dots \rangle$. Electrons bunched at π provide maximum gain where as electrons bunched at $\pi/2$ provide minimum gain.

The dimensionless current j provides the coupling between the electron beam and the light wave. The response of the optical wave to bunching in the beam is also determined from j . By comparing the magnitudes of the dimensionless quantities to certain threshold values, a simple identification of FEL gain regimes can be made [Ref. 5]. When $j < 1$, the FEL gain is low with non-exponential growth. When $j > 1$, the FEL gain is high with exponential growth. For values of j not within

either of these regimes, the gain does not have either of these distinctive features. The proposed compact FEL design has dimensionless current $j=5$. Therefore, the correct theoretical approach to analyzing gain for this device must be carefully chosen. A discussion of the methods used to evaluate gain is addressed in Chapter IV.

D. STRONG OPTICAL FIELDS AND SATURATION EFFECTS

The Maxwell-Lorentz theory of the FEL combines Maxwell's wave equation for the optical wave and the relativistic Lorentz force equation for the electrons to describe laser dynamics in both strong and weak optical fields. The extension of this theory into the strong field regime allows the use of the optical wave and electron pendulum equations to accurately study the electron phase-space evolution and gain in the FEL [Ref. 5]. This extension is allowed because both equations assume there are no significant changes in the electron energy γmc^2 . This implies the electron energy is not followed self-consistently. Strong optical fields can be reached after many passes in a low-gain oscillator, or at the end of a high-gain amplifier. When the optical field in either the low or high-gain system becomes sufficiently strong, the initially uniform electron beam becomes overbunched and complicates the electron phase distribution $f(\zeta, v)$. Overbunching is the process where electrons become overpopulated at the end of the laser and do not efficiently drive the optical wave. This over-bunching can destroy the

coherent bunching responsible for the initial gain, and indicate the onset of saturation and the reduction of gain.

Strong fields begin when $|a| \approx \pi$. Recalling the electron pendulum equation, $\dot{\zeta} = \dot{\zeta}^0 = |a| \cos(\zeta + \phi)$. We see that a bunch formed at the proper phase for gain, $\zeta + \phi \approx \pi$, would soon evolve by $\Delta\zeta \approx -|a| \approx -\pi$ to the phase for absorption $\zeta + \phi \approx 0$. The electron phase velocity is proportional to the rate of energy transferred from the electron bunch and determines the amount of power transferred into the optical wave. Similarly when $\zeta + \phi \approx -\pi$, the electron phase velocity v and rate of energy transferred from the bunch is positive implying that energy is being extracted from the optical wave decreasing the gain. The strong fields cause the electron bunch to move too far along the phase-axis in phase-space and cause the electron phase to shift to a relative phase for absorption. The electrons become trapped in closed phase-space orbits as some electrons can overtake, or fall behind other electrons in the beam.

An estimate of how much energy can be lost by the electron bunch in strong fields can be made by looking at the phase-space diagram. Figure 7 shows the FEL phase-space evolution for weak fields and low current where the pendulum and optical equations are solved numerically in an optical field $a_0=2$ and $j=1$. Electron phase velocity v verses electron phase ζ describes the evolution of electrons within an optical wavelength. Shown in the figure are 20 electrons; each electron's initial conditions determine the evolution of its velocity $v(\tau)$ and position $\zeta(\tau)$. Each electron is therefore constrained to follow a particular path in phase-

space. The final phase-space positions of the electrons are drawn in (ζ, v) . The separatrix path separates open orbits from close orbits. The height of the closed-orbit region is determined by the optical field strength and ultimately determines the laser gain process. The two plots to the right in the figure represent the evolution of the gain G and optical phase ϕ from the beginning to the end of the undulator.

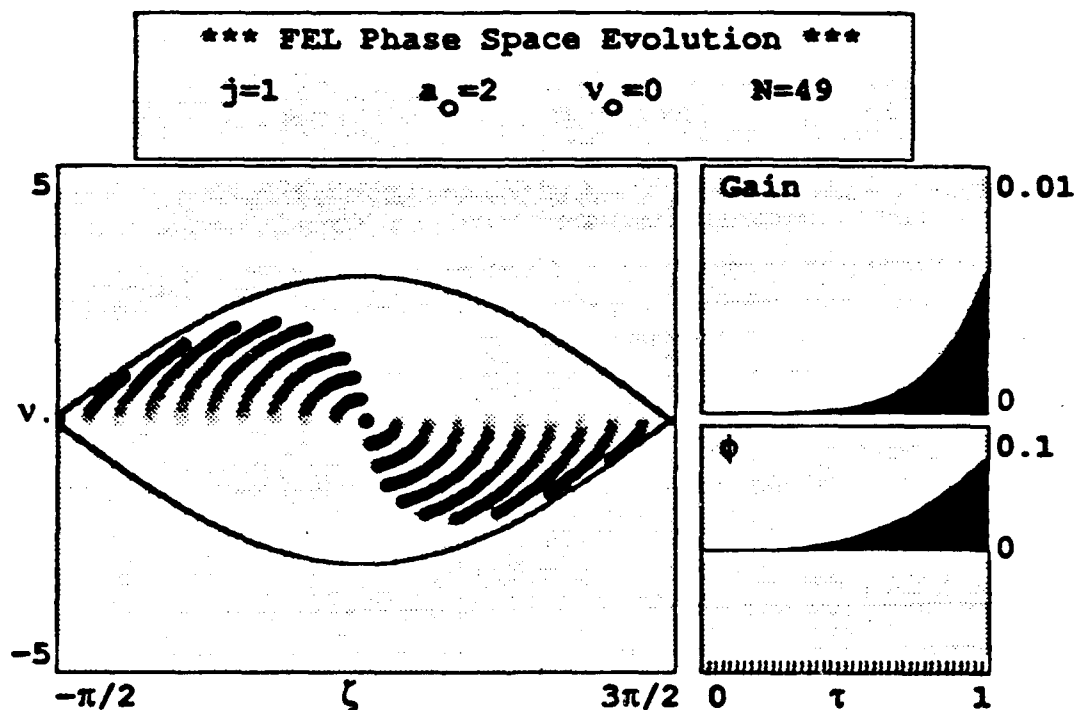


Figure 7. Phase Space Diagram for Weak Fields with Low Current.

The electrons are initially positioned such that work is done on them; they gain energy and move ahead of the average flow at the top of the phase-space picture. Other electrons lose energy to the radiation field, and move back behind the average flow to cause bunching. At $\tau \approx 1$, there is no gain or phase shift from

the uniform spread electron beam, but as bunching develops the gain and optical field increase. The maximum energy of the electron bunch occurs when electrons are positioned at the highest point on the separatrix-axis, and similarly, the minimum energy occurs when the electrons are located at the lowest point of the v -axis. The total energy that the electron bunch can transfer to the optical wave is therefore estimated by the height of the separatrix path, $4|a|^{1/2}$ from peak-to-peak.

Figure 8 shows the compact FEL phase-space evolution for weak fields with moderate current where the pendulum and optical equations are solved numerically in an optical field $a_0=2$ and $j=5$. The electrons start outside the closed orbits and evolve into a bunch at $\zeta \approx \pi$. The optical amplitude is driven by this bunch and drives the gain by a factor of 100 higher than the previous case $j=1$.

When $|a| \approx \pi$ at saturation, the change in the phase velocity is $\Delta v(\tau) \approx 4|a|^{1/2} \approx 2\pi - \frac{\Delta\gamma}{\gamma} \approx \frac{1}{2N}$, and corresponds to a change in the bunch's energy by $\Delta v \approx 4\pi N \Delta\gamma / \gamma \approx 2\pi$. A change in phase velocity by 2π can cause the electron bunch to shift from peak gain to peak absorption.

Figure 9 shows the compact FEL phase-space evolution for strong field $a_0=20$, with moderate current $j=5$. Due to the strong fields and the rapid rate of bunching near the beginning of the undulator, the gain and phase begin to grow rapidly. At about $\tau \approx 1/2$, the optimum relative phase $\zeta + \phi \approx \pi$, for gain occurs resulting in the best spatial overlapping of the electrons. However absorption occurs as the bunch evolves further past this optimum phase to $\zeta + \phi \approx 0$. The gain

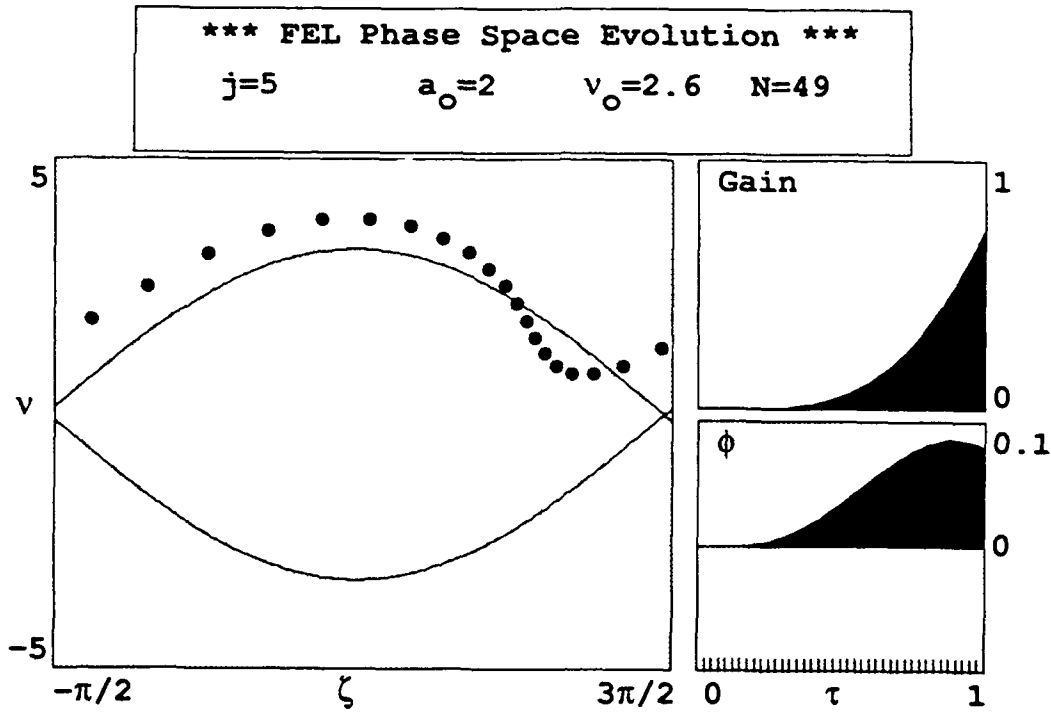


Figure 8. Phase-Space Diagram for Weak Fields with Moderate Current.

is seen to first peak, and then decrease as the overbunched electron beam drives the optical wave and continues to evolve so that energy flows back into the electron beam. The final gain, $G \approx 10\%$, is significantly reduced from the theoretically possible, $G = 0.135j$, in weak optical fields.

As anticipated, the FEL interaction in strong optical fields demonstrates significantly different characteristics upon saturation. The gain spectrum, $G(v_0)$, changes shape in the presence of strong fields. As discussed in the gain mechanism section, the gain spectrum in weak fields and low-current is anti-symmetric about the resonance wavelength with a peak gain $G = 0.135j$, at phase velocity $v_0 = 2.6$ and has a gain bandwidth of roughly $\Delta v_0 = \pi$. Similarly the peak

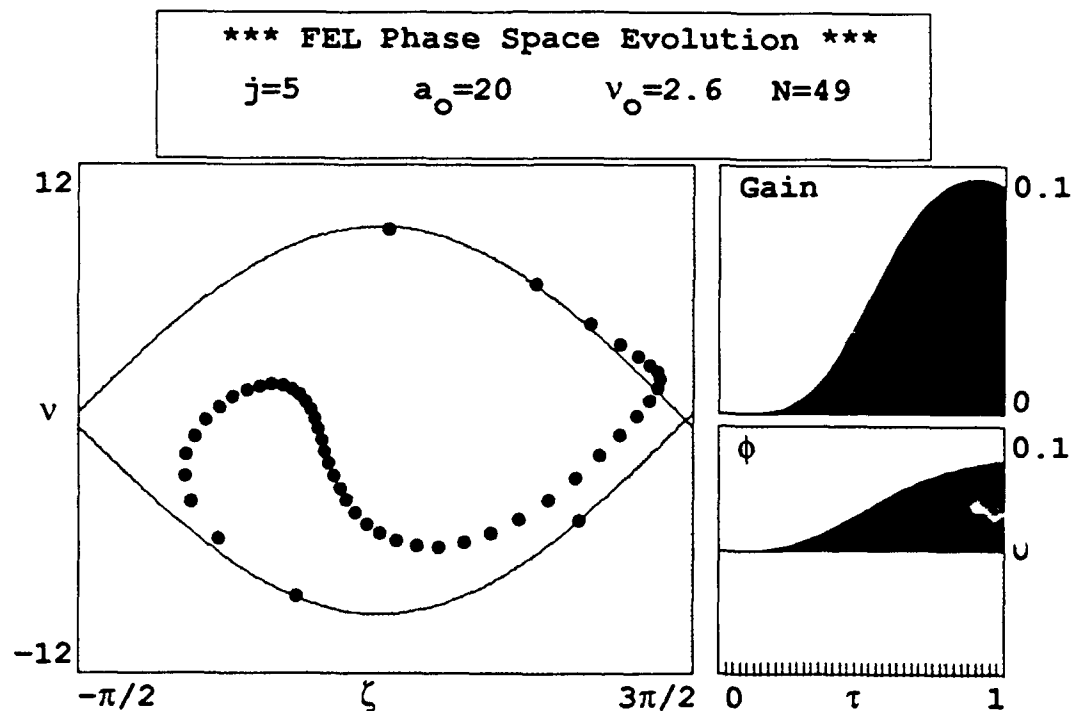


Figure 9. Phase-Space Diagram for Strong Fields with Moderate Current.

absorption occurs at the phase velocity $v_0 = -2.6$ with a value of $G = -0.135j$. For $j=5$, the gain spectrum is shifted slightly to the left away from resonance. As the initial field strength increases, the peak gain decreases and the wavelength at which peak gain occurs also increases away from resonance. The gain spectrum width becomes broader and distorts as the FEL saturates. The gain is further reduced as the bunched electrons move out of resonance and lose energy to the optical field. These effects are shown in Figure 10 where the gain spectrum $G(v_0)$ for moderate current $j=5$ and initial field strength $a_0=0$ is increased to 30. The phase velocity that gives peak gain increases away from resonance as the field

strength a_0 increases. The gain describing the interaction after each pass in the FEL oscillator causes the optical field to grow a little stronger as can be seen along the a_0 -axis. As the power grows over many passes, typically several hundred passes are required to evolve from the weak-field to the strong-field regime near saturation, the optical wavelength is observed to shift to longer wavelengths corresponding to a larger initial phase velocity.

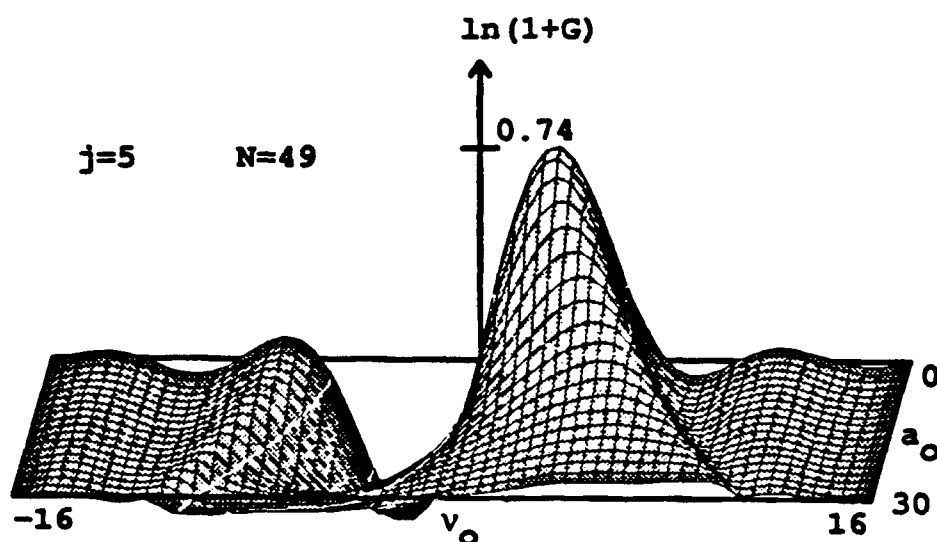


Figure 10. The Gain Spectrum $G(v_0)$ for Moderate Current with Increasing Optical Field Strength a_0 .

E. PRODUCTION OF HIGHER FREQUENCY HARMONICS IN FELs

The frequency of radiation emitted by a relativistic electron traveling through a linearly-polarized undulator is given by $n\omega = \omega_0(1 + K^2)/2\gamma^2$. Here, $n=1,3,5,\dots$

is known as the harmonic number. The fundamental is defined as the frequency produced when $n=1$ [Ref. 11]. We address an overview of the harmonic mechanism to provide an intuitive understanding of their origin so specific compact designs that operate on harmonics can be explored in Chapter IV. Using numerical methods. Chapter IV will also examine the advantages of using harmonics in compact FELs. Here, dynamics of relativistic electrons in the presence of light, stimulated emission, are generalized to describe higher harmonics of the optical field [Ref. 6,12]. Harmonics are produced by extra oscillations of the electron that occur at each undulator period. The energy transferred between the electron beam and light, given in (10), is extended to include this motion.

Harmonics result from a coupling between electrons and light due to an alteration of the energy transfer mechanism. In addition to the transverse sinusoidal motion of electron trajectories in the linearly-polarized undulator, a small periodic longitudinal motion exist that cause spontaneous emission and gain in odd multiples of the fundamental, $n\omega = nkc$. The harmonic coupling is due to the time electrons spend in periodic, longitudinal motion while transferring energy to the optical wave. A weighted coupling between electrons and light is expressed by Bessel functions which modify the undulator parameter K . The modified undulator parameter provides a convenient method of incorporating harmonics in the optical wave equation, electron pendulum equation and gain analysis. An

outline of how this modified undulator parameter is derived and incorporated into (10) is given below.

The ideal undulator field is given by

$$B_u = B(0, \sin(k_o z), 0). \quad (43)$$

The components of the Lorentz force equations including this new undulator field are

$$\frac{d}{dt}(\gamma \beta) = -\frac{e}{mc}(\beta \times B_u) = \frac{-eB}{mc}(-\beta_z \sin(k_o z), 0, \beta_x \sin(k_o z)) \quad (44)$$

$$\frac{d\gamma}{dt} = 0 \Rightarrow \gamma = \text{constant}. \quad (45)$$

The x and y-velocities are found by integrating the respective component equation:

$$\beta_x = \frac{\sqrt{2}K}{\gamma} \cos k_o z + \delta \beta_{x_c} \quad (46)$$

$$\beta_y = \text{constant} + \delta \beta_{y_c} \quad (47)$$

where $K = e\bar{B}\lambda_o / 2\pi mc^2$ and $\delta \beta_{x_c}$ and $\delta \beta_{y_c}$ are constants of integration. Using $\beta_z^2 = 1 - \gamma^{-2} - \beta_x^2 - \beta_y^2$, (46) and (47), and assuming perfectly injected electrons with $\delta \beta_{x_c} = \delta \beta_{y_c} = 0$, the electron z motion is given by

$$\beta_z^2 = 1 - \gamma^{-2} \left[(1 + K^2) + K^2 \cos(2k_0 z) \right]. \quad (48)$$

At $z=0$, the injected z velocity is

$$\beta_z^2|_{z=0} \equiv \beta_z^2(0) = 1 - \gamma^{-2} (1 + 2K^2) \quad (49)$$

$$\beta_x|_{z=0} \equiv \beta_x(0) = \frac{-K}{\gamma} \quad (50)$$

for perfect injection.

Now (48) can be written

$$\beta_z^2 = \beta_z^2(0) + \left(\frac{K}{\gamma}\right)^2 - \left(\frac{K}{\gamma}\right)^2 \cos(2k_0 z) \quad (51)$$

and perturbation expansion in $(K/\gamma)^2$ is now possible. Defining $\beta_z(t) = \bar{\beta}_z + \Delta\beta_z(t)$, the z motion to order $(K/\gamma)^2$ is derived from integrating z to lowest-order to give:

$$\beta_z^2 = \bar{\beta}_z^2 - 2\left(\frac{K}{\gamma}\right)^2 \cos(2k_0 z). \quad (52)$$

To lowest order in $(K/\gamma)^2$, $[\beta_z = z/c = \beta_z = 1 - 1/2(1 + K^2)]$ so that the electron position can be written as the expansion $z = z_0 + \beta_z ct + \dots$. The integrated z motion, becomes

$$z(t) = (z_0 + \bar{\beta}_z ct) - \frac{\lambda_0}{16\pi} \left(\frac{K}{\gamma}\right)^2 \sin((2k_0 z_0) + 2\beta_z \omega_0 t). \quad (53)$$

The first two terms express the slowly evolving motion of the electron along the undulator-axis. The last term expresses the fast, periodic, longitudinal motion on

the optical wavelength scale and causes higher harmonics. This oscillatory motion occurs once per undulator period. Variations of the fundamental electric field observed by the electron as it travels through a undulator period causes the nonuniform axial motion. The fast and slow motions can now be expressed as

$$z(t) = \bar{\beta}_z ct - \frac{\lambda_o}{16\pi} \left(\frac{K}{\gamma} \right)^2 \sin(2\omega_o t) \text{ where } z_o = 0 \text{ and } \bar{\beta}_z = 1. \quad (54)$$

Defining $\xi = K^2 / 2(1 + K^2)$, (54) can be expressed as

$$z(t) = \bar{\beta}_z ct - \frac{\xi}{K} \sin(2\omega_o t). \quad (55)$$

Substitution of (55) into (10) and recalling $\zeta = (k + k_o)z - \omega t$ is the electron phase, the electron energy equation is written explicitly in terms of fast and slow variables:

$$\begin{aligned} \dot{\gamma} = \frac{eKE}{2\gamma mc} [& \cos(n\zeta + \phi - (n-1)\omega_o t - n\xi \sin(2\omega_o t)) \\ & + \cos(n\zeta + \phi - (n+1)\omega_o t - n\xi \sin(2\omega_o t))] \end{aligned} \quad (56)$$

Using the generating function to expand sinusoidal terms in cylindrical Bessel functions and averaging over one undulator period, (56) is written as

$$\dot{\gamma} = \frac{e\mathfrak{R}_n(\xi)EL}{2\gamma mc^2} \cos(n\zeta + \phi)$$

where

$$\mathfrak{R}_n(\xi) = K(-1)^{(n-1)/2} [J_{(n-1)/2}(n\xi) - J_{(n+1)/2}(n\xi)] \text{ for } n = 1, 3, 5, \dots$$

The product of the undulator constant and the Bessel functions provides a convenient mathematical notation to compare FEL operation in any selected

harmonic. By using the theory already developed in the preceding sections the generation of harmonics can be expressed by simply replacing $K - \mathfrak{K}_r(\xi)$.

III. CONCEPT OF A COMPACT FEL

To increase the accessibility of FEL's to a broad range of users a reduction in size and complexity of FEL systems must be pursued. The largest component of a FEL system is usually the electron accelerator due to the large electron energy required. The relatively large electron beam energy along with high current requires significant radiation shielding for personnel safety and therefore increasing the overall weight of the FEL system [Ref. 8]. To reduce these requirements, FELs that operate on harmonics have been proposed to allow using lower energy electron beam. This effect can be examined by considering a fixed undulator design, and referring to the resonance condition given in [Ref. 12], $n\lambda = \lambda_o(1 + K^2)/2\gamma^2$, where the harmonic number n is included. The undulator design depends on the period λ_o and undulator parameter K and therefore assumed to be constant. For a desired optical wavelength, the only variables in the resonance equation are the Lorentz factor γ and harmonic number n . By increasing n , we see γ can be reduced accordingly, provided λ_o , K and λ remain fixed. Since γ is proportional to the electron beam energy, using harmonics can provide a viable method of designing compact FELs which require lower energy.

A. DEVELOPMENT OF THE PHOTO-CATHODE INJECTOR

Preliminary design studies have been conducted at Los Alamos National Laboratory (LANL) on an infrared compact RF-linac driven FEL [Ref. 8] that relies upon two technological advances:

- a very bright electron beam from a photo-cathode injector, and a
- pulsed-wired technique for short-period high-field undulators.

The photo-cathode injector, designed by Sheffield and Fraser at LANL, is a compact device used to generate the FEL's electron beam [Ref. 13,14]. The device uses a light-activated, photo-emissive electron source in order to provide excellent control of the electron distributions. Electron distribution functions determine the quality of the electron beam, and play a significant role in the small-signal gain that is available from a given undulator. Beam quality can be described by two effects, emittance and energy spread [Ref. 5]. Both effects reduce FEL performance by degrading the bunching process described earlier. The transverse emittance is used to describe the imperfect FEL injection of electrons off-axis in either position or angle. Since the transverse coordinates of the electrons in the FEL are (x,y) , we must consider electron injection off-axis to include both dimensions. Figure 11, however, shows the electron's injection only in the y -direction. A similar schematic holds for the x -direction.

An imperfectly injected electron has a decrease in phase velocity, and random spreads in (y_o, θ_{y_e}) and (x_o, θ_{x_e}) . These effects will begin to decrease

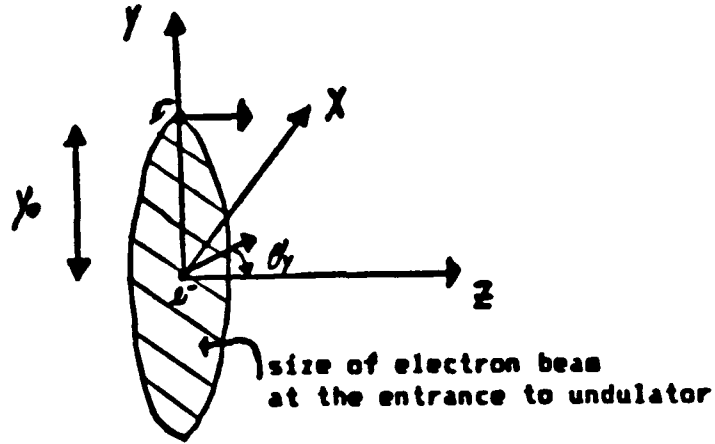


Figure 11. Schematic of Injection of Imperfect Electrons Into Undulator. Injection of imperfect off-axis into the undulator due to spread of position y_0 and angle θ_y .

the FEL's ability to bunch electrons causing a decrease in gain. Assuming the motion of the electrons in the two x and y transverse directions is independent, a transverse phase-space plot can be constructed. Taking the electron distribution to be a product of uncorrelated Gaussians in angular spreads and positions, the transverse emittance, ϵ_y and ϵ_x , are defined by the corresponding phase-space areas. See Figure 12.

$$\epsilon_y = 2\pi y_0 \theta_y, \quad \epsilon_x = 2\pi x_0 \theta_x, \quad (57)$$

An ellipse drawn around the electron particle distribution defines an area in y - θ phase space that characterizes the transverse emittance. Similar results hold in x - θ phase space.

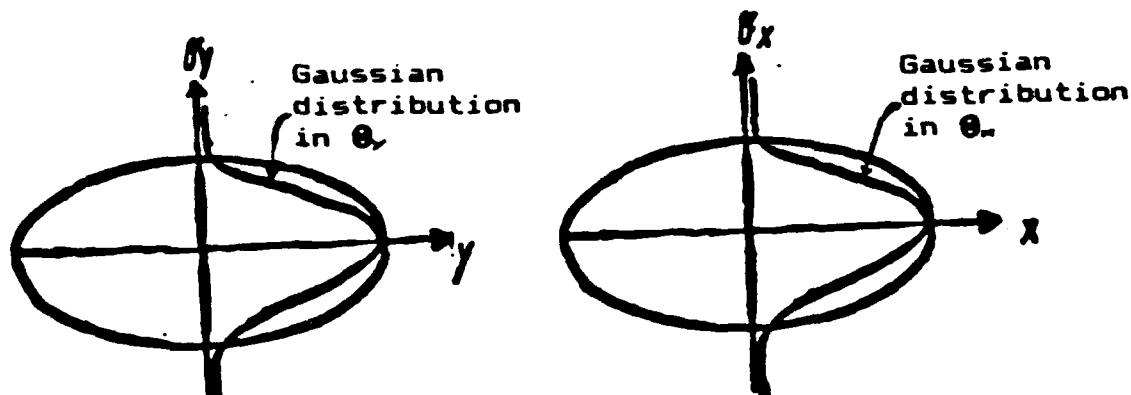


Figure 12. Electron Particle Phase-Space Distribution.

An ellipse drawn around the electron particle distribution defines an area in $y-\theta_y$ phase space that characterizes the transverse emittance. A Gaussian distribution of positions occur in y with an uncorrelated Gaussian distribution of angles in θ_y . Similar results hold in $x-\theta_x$ phase space.

The emittance growth of the beam is reduced by using the photo-injector design, because the electron bunch produced from the cathode is rapidly accelerated to relativistic energies in a single cavity, thereby reducing significantly the electron beam transport at low energies [Ref. 13,14]. The desired low emittance is also required for the electron beam to propagate through the small gap in the undulator, and the optical mode in the resonator cavity. Brightness, a property of the electron beam, is proportional to the current and inversely proportional to the beam quality [Ref. 15]. This implies emittance must be reduced in order to obtain an intense, bright electron beam.

B. TECHNOLOGICAL ADVANCES IN MICRO-UNDULATOR DESIGNS

Warren and Feldman [Ref. 16] discuss the design and construction of iron-free electromagnets driven by pulsed high-currents. The micro-undulator can generate the high magnetic fields needed to reduce the period, and still maintain optical gain at reasonable values. These devices have periods of less than one centimeter and can be used to generate light at short wavelengths with electron beams of only moderate energy. While reducing the period, the designer requires the undulator parameter, K , to be less than one in order to extract the maximum gain from the FEL. Pulsed currents in copper-like conductors, that produce current densities in excess of about 10^3 A/cm², can be utilized to accomplish this requirement. Limits of this technology involve undulator construction errors, material stresses and electron beam alignment issues [Ref. 17]. Compared to other undulator technologies, this design has the greatest potential to reach short FEL wavelengths with reduced electron beam energy.

The harmonic mechanism in FELs, discussed in the last chapter, is the result of the fast, periodic axial motion of the electrons. The effects of harmonics can be manipulated by designing micro-undulators that operate with periods which are multiples of the fundamental period. Re-writing the resonance condition for harmonics as $\lambda = \lambda_0 (1 + K^2) / 2 \gamma^2 n$, it can be shown harmonics of the undulator's period can be utilized to design micro-undulators. These designs would have fewer periods and still have the requirements mentioned earlier.

The top schematic of Figure 13 illustrates an FEL operating on the fundamental, $n=1$, for a fixed undulator and fixed electron beam energy. In the fundamental, the undulator has a period λ_0 , undulator parameter K , and initial electron velocity corresponding to a Lorentz factor, γ . The fundamental optical wavelength, λ , is found from the harmonic resonance condition with $n=1$. The middle schematic illustrates the same undulator design and electron beam energy, but the third harmonic, $n=3$, is used. The resulting wavelength is $\lambda/3$ or one third the fundamental wavelength satisfying the harmonic resonance condition with $n=3$. This is the conventional use of harmonics to reduce the optical wavelength. A new method of utilizing harmonics proposed by R. Warren, is shown at the bottom. Using the same electron beam energy and undulator parameter K , the optical wavelength, λ , is acquired from the harmonic resonance condition when the undulator period is increased to three times the fundamental's undulator wavelength $3\lambda_0$. The advantage of this design is that the micro-undulator FEL can reach short optical wavelengths with a reasonable undulator period and a low energy electron beam. The next chapter discusses in detail three specific micro-undulator designs that utilize harmonics in this fashion.

Undulator parameter K
and electron beam energy
remain fixed

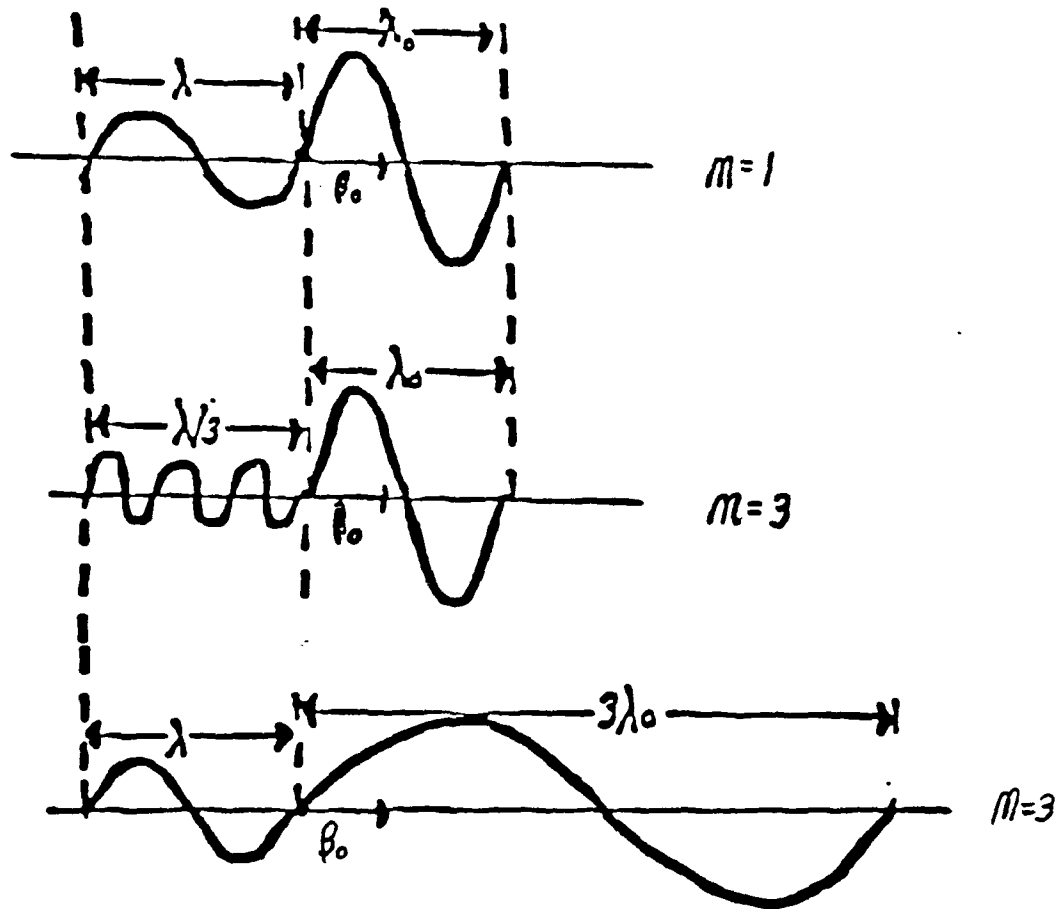


Figure 13. Schematics of Compact FEL Operating on Optical and Undulator Harmonics.

IV. EVALUATION OF COMPACT FEL OPERATION

A. HIGHER HARMONIC GENERATION IN COMPACT FELs

There is currently interest in lasing on higher harmonics of the fundamental frequency in order to reach optical wavelengths in the range of 0.4 to 0.5 microns with an electron beam energy of about 20 Mev. The use of harmonics at short wavelengths allows a realistic undulator parameter, since the undulator's length is shorter, the number of periods is less and longer periods would be used. The consequence would be a micro-undulator design that would be easier to fabricate. Shorter undulators would also minimize the penalty from emittance and energy spread inherent in all realistic electron beams [Ref. 18]. For a fixed optical wavelength, λ , and an undulator design using higher harmonics, the energy of the electron beam, γmc^2 , can be reduced thereby lowering the radiation shielding requirements for personnel. Operation over a wider range of wavelengths, and the increase in optical power at saturation provide additional benefits of using higher harmonics in compact FELs [Ref. 12]. The gain that can be achieved using various harmonics depends on electron beam properties, beam quality factors, and the specific micro-undulator design chosen. To evaluate gain on harmonics for new FEL design systems, it is necessary to utilize computer codes that represent the mathematical formulation of the FEL equations discussed in Chapter II.

B. FEL SIMULATION METHODS

Various numerical simulation methods, essential to relating the three major technologies of optics, relativistic electron beams and undulator magnets have been developed to analyze and design RF-linac-driven FELs [Ref. 19]. Numerical calculations using five methods that model FEL laser physics with different levels of sophistication and mathematical formalism are conducted on three micro-undulator designs. The designs are explored to demonstrate the use of higher harmonics in order to reach optical wavelengths with lower electron beam energy. These preliminary compact FEL designs were proposed by R. Warren at LANL. The design method is based on Dattoli's parameterized gain formula [Ref. 20] and approximate solutions for the magnetic fields of single and double-current carrying helical windings [Ref. 21]. The intent of the design code is to accurately model gain characteristics, and provide a basis within which micro-undulator parameters can be developed in order to optimize compact FEL operation. The assumptions, approximations, regions of validity and definitions of important parameters for the methods used in the analysis will be discussed through this chapter.

C. COMPACT FEL DESIGN PARAMETERS

The electron beam current and energy spread, and the optical wavelength are the same for all three micro-undulator designs evaluated. The electron beam has current $I=400$ A, and Lorentz factor $\gamma=40$ corresponding to an energy of about 20 MeV. The beam emittance is varied from $\epsilon=\lambda/4$ to $\epsilon=7\lambda$, while the

Gaussian energy spread varies from 0% to 0.8%. The optical wavelength is $\lambda = 0.4$ microns with the optimum Rayleigh range $z_o = L / \sqrt{12}$ where L is the length of the undulator. Two of the three undulators are designed to be operated on higher harmonics with undulator periods in the range of $\lambda_o = 0.3$ to 0.5 cm. The values of the harmonic number, number of periods, period, and undulator parameter are given for the three micro-undulators in Table I.

TABLE I.

	FUNDAMENTAL	THIRD HARMONIC	NINTH HARMONIC
n	1	3	9
N	413	49	19
$\lambda_o(\text{cm})$.013	0.33	0.54
K	0.018	0.408	0.540

D. GAIN DEGRADATION DUE TO BEAM QUALITY AND THE FILLING FACTOR

An analysis of beam quality and the filling factor \mathcal{F} is necessary for a discussion of the FEL gain evaluation. Emittance and energy spread effects that describe beam quality, introduced in Chapter III, are discussed in greater detail to show important FEL design limits. The filling factor \mathcal{F} , defined as "the ratio of the electron beam size πr_e^2 " to the "optical mode size πw_o^2 ," is used to define a limit on the electron beam area. [Ref. 5]

Gain in the FEL depends on details of the phase velocity distribution where the ability to bunch electrons is diminished in a different way for each shape [Ref. 22,23]. The exact distribution function of the electrons transverse motion depends on the construction and operation of the accelerator and usually is not known exactly. The distribution for initial electron energies perfectly injected into the undulator is represented by the normal distribution function [Ref. 23]

$$f_G(v) = \frac{\exp[-(v - v_o)^2 / 2\sigma_G^2]}{\sqrt{2\pi} \sigma_G} \quad \text{for all } v \quad (58)$$

where $f_G(v)$ = Gaussian distribution
 v = phase velocity
 v_o = peak phase velocity
 $\sigma_G = 4\pi N \Delta\gamma/\gamma$ is the standard deviation of v away from the peak phase velocity v_o .

A Gaussian distribution of angles about the z-axis is given by the exponential distribution function [Ref. 23]

$$f_\theta(v) = \frac{\exp[-(v_o - v) / \sigma_\theta]}{\sigma_\theta} \quad \text{for } v < v_o \quad (59)$$

$$f(v) = 0 \quad \text{for } v > v_o$$

where $\sigma_\theta = 4\pi N \gamma^2 (\Delta\theta / 1 + K^2)$
 $\Delta\theta$ = standard deviation of angular distribution
 v_o = phase velocity for electrons entering on-axis.

It is important to note that for any angular-spread of phase velocity, the longitudinal velocities of these electrons are decreased. The phase velocity is skewed only in the negative direction indicating that the electron's energy can only be decreased regardless of the initial angle relative to the z-axis.

The decrease in phase velocity for an imperfectly injected electron is given by [Ref. 5].

$$\Delta v = \frac{2\pi N}{1 + K^2} (K^2 k_o^2 r_o^2 + \gamma \theta_{y_e}^2) \quad (60)$$

where Δv = change in electron's phase velocity, and
 θ_{y_e} = electron's initial injection angle.

Any change in the electron's average z-velocity causes a change in the electron's phase velocity as given by the above expression. When the electrons are injected off-axis in either position or angle, they experience a field strength that is stronger than the field strength on the central-axis. This effect causes the electrons to be focused back toward the center line, and execute a number of betatron oscillations, $N_\beta = NK / \gamma$, in the transverse x-y plane. The betatron oscillations result from transverse excursions of electrons that have a constant of motion defined by a harmonic potential [Ref. 5]. In the situation where the electron beam is guided into this betatron motion, it is desirable to match the angular and position spreads so that the beam does not focus or expand as it travels along the z-axis. A smooth propagation of the electron beam with minimum spread in the phase velocities is achieved by requiring that the angular and position spreads be matched [Ref. 5]:

$$K k_o r_o = \gamma \theta_y \quad (61)$$

where θ_y is now a spread in angles.

The spread of electron phases accumulated over the undulator length in a matched beam is given by [Ref. 5]

$$\Delta v = \frac{4\pi N}{1+K^2} K^2 k_o^2 r_e^2. \quad (62)$$

If we require the phase spread not exceed an optical wavelength at the end of the undulator, $\Delta z/\lambda \leq 1$ the limit for r_e is found.

Relating Δv to $\Delta z/\lambda$ at the end of the undulator we first find $\Delta \zeta = \Delta v$ at $\tau=1$, since $v = \zeta$. Recalling $\Delta \zeta = k \Delta z$, the phase spread can be written as $\Delta v = k \Delta z$. Eliminating Δz from $\Delta z/\lambda > 1$ and $\Delta v = k \Delta z$, and using (62) we find the phase spread limit can be written as

$$\frac{4\pi N}{1+K^2} \frac{K^2 k_o^2 r_e^2}{K} \leq \lambda. \quad (63)$$

Using the resonance condition, $N_b = NK/\gamma$ and $L = N\lambda_o$, the limit for r_e is found to be

$$\pi r_e^2 \leq \frac{nL\lambda}{4\pi^2 N_b^2}. \quad (64)$$

This resulting limit on the electron beam area is to insure that the phase spread does not degrade beam quality.

An important limit of the electron beam radius constrains the electron beam to be inside the optical mode $r_e \leq w_o$. The fraction of the beam outside the mode cannot participate in the gain process. The expansion of a coherent beam with a Gaussian intensity profile in the fundamental mode is given by [Ref. 24]

$$w^2(z) = w_o^2 \left[1 + \left(\frac{\lambda (z - L/2)}{\pi w_o^2} \right)^2 \right] \quad (65)$$

where $w(z)$ describes the beam contour at position z , and w_o the waist spot size at $z=0$.

The Rayleigh range, defined as $z_o = \pi w_o^2 / \lambda$, is the distance where the optical transverse mode expands to twice the size compared to waist size in the undulator [Ref. 5]. See Figure 14. The Rayleigh range is optimized by minimizing the optical mode volume around the electron beam. The optical mode volume is calculated by integrating the beam intensity profile along the entire length of the undulator [5].

$$V = 2 \int_0^{L/2} \pi w_o^2 \left(1 + \frac{z^2}{z_o^2} \right) dz = \lambda L \left(z_o + \frac{L^2}{12 z_o} \right), \quad (66)$$

where $\lambda = \pi w_o^2 / z_o$.

The two limiting cases, $z_o \rightarrow 0$ and $z_o \rightarrow \infty$, each result in an optical mode volume that tends to infinity. In the first case, a small waist is pinched in the middle of the optical mode, and rapidly expands due to diffraction. An infinite volume means that light at the ends of the undulator would be far from the electron beam and would not be significantly amplified. In the second case, a plane wave would develop where all of the optical mode is large. The optical mode would be far away from the electron beam at the end of the undulator and at the waist, as well. Both these cases are unsuitable for any physical solution therefore there must be an optical mode volume minimum between 0 and ∞ .

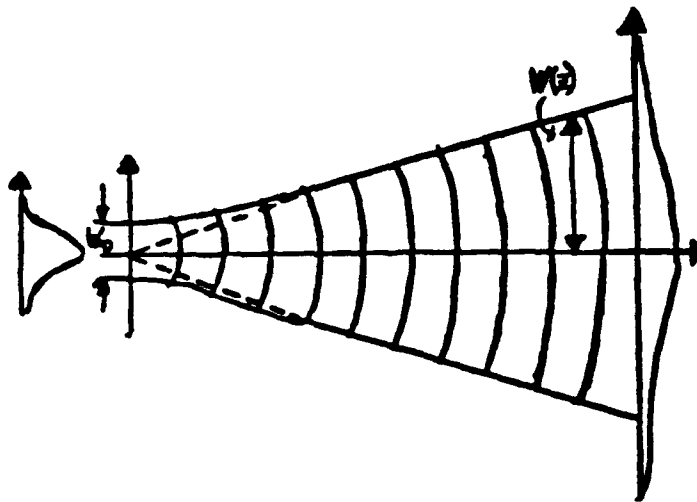


Figure 14. Schematic for Diffraction of Light Wave in Undulator.
Schematic for a Gaussian beam in lowest-order expanding due to diffraction spreading as it propagates away from the waist region located at center of the undulator.

We find the value of z_0 that make the volume of the optical mode a minimum [Ref. 5]. Setting the derivative of (66) to 0

$$\frac{dV}{dz_0} = \lambda L \left(1 - \frac{L^2}{12 z_0^2} \right) = 0 \quad (67)$$

the optimum Rayleigh range is found to be $z_0 = L / \sqrt{12}$. By making the Rayleigh range equal to about a third to a fourth the undulator, the minimum optical mode volume is found. This characteristic volume provides the optical mode for maximum gain.

For the optimum Rayleigh range, $r_0 \leq w_0$, gives a limit to the electron beam area

$$\pi r_e^2 \leq \frac{L\lambda}{\sqrt{12}} \quad (68)$$

When this condition is satisfied, the small-signal gain is independent of the electron beam size, and depends only on the current contained within the optical mode. Emittance, the product of the rms values of the angular and radial position spreads, provides the fundamental limit to beam size and determine a corresponding spread in the longitudinal electron phases. Comparing the restrictions (62) and (66) shows that for $N_b \leq 1$, the only effect of emittance occurs when the electron beam is larger than the optical mode, or simply $F \geq 1$. This restriction simplifies the analysis of any FEL.

E. METHODS OF ANALYSIS

1. Three-Dimensional Simulation Codes

a. FELEX

FELEX, further abbreviated to FEX, numerically calculates three dimensional particle motion and optical diffraction effects [Ref. 25]. The computer code is based upon the Monte Carlo technique that simulates three dimensional FEL physics by following orbits of simulation electrons; 2,560 are used in our analysis to determine the optical field interaction. Numerical solutions to the FEL equations (5a), (5b), and (6) are found using three major algorithms [Ref. 25], (i) a set of ordinary differential equations describing the electron motion, (ii) a parabolic partial differential equation governing the optical field, and (iii) the

connection between the optical field and the electron motion through a source term that is a function of the electron current density. The currents from the set of electron equations provide the source term in Maxwell's equations and connect the electron motion to the optical field [Ref. 25]. Averaging the relativistic Lorentz force equation (1) over the spatial period of the undulator, the numerical solution is acquired that incorporate in the dynamics (i) finite emittance, (ii) energy spread, and (iii) linear undulator focussing of the electron beam in the undulator field. The program was set up for curved-faced pole undulators where equal focusing in the x and y-directions is obtained. This effect causes the electron beam to remain round as it travels through the undulator instead of being focused only in one direction, and thereby, developing an elliptical shape. In short undulators, which are considered here, gain calculations are not substantially affected by the fact that the simulation code uses curved-faced poles instead of flat-faced poles. These are single wavefront calculations that do not consider the pulse nature of both the electron and optical beam. Optical gain and refractive effects are "self-consistently" calculated as the light interacts with electrons inside the undulator. A finite width of the optical wavefront near the center of the optical pulse length is modeled. The transverse profile of the electric field is set equal to a normal Gaussian mode characterized by a wavelength, focal position, and a Rayleigh range. The optical field at the exit of the undulator is propagated through the optical resonator to the entrance of the undulator where the next electron pulse interacts to simulate an

FEL oscillator. The evolution of the optical field is found by solving the paraxial wave equation [Ref. 25,26], since FEX models the optical components of the resonator by thin lens. The paraxial wave equation, derived from the formulation for the optical wave equation discussed in Chapter II, has an inhomogeneous driving term that is a result of the stimulated emission of the electron beam when placed in the optical field. An extension of the FEX code was made at LANL to incorporate a model of coherent spontaneous emission of harmonics in the FEL oscillator operating at high power at the fundamental wavelength with a plane polarized undulator. An additional modification allows calculations of undulator field errors due to manufacturing flaws in magnetic material or imperfect alignment during construction [Ref. 26].

b. Wavefront simulation

A wavefront simulation, WFS, numerically solves the 3-D parabolic wave equation, together with the pendulum equation [Ref. 5]. This method includes most of the FEL effects incorporated into FEX except that a monoenergetic electron beam is assumed. When the gain is sufficiently high, the electron beam can distort the optical mode into a combination of resonator modes [Ref. 5]. This code accounts for distortion by self-consistently calculating the optical field for high gain in 3-D without using the filling factor. Harmonic coupling and strong fields are included in the code.

2. One-Dimensional Simulation Code

Numerical solutions of the wave and pendulum equations, SIM, for both strong and weak fields are found with approximately 1000 simulation electrons. This analysis includes the filling factor, harmonic coupling and electron beam degradation effects. The evaluation of the FEL interaction is described by the dimensionless current j which determines the response of the optical wave to bunching in the beam [Ref. 5].

3. Analytical Methods

a. Integral Equation

Combining the electron pendulum and optical wave equations in weak fields, an integral equation, INT, governs the evolution of the optical field [Ref. 5,22]. This development allows the evaluation of gain degradation from a Gaussian electron beam distribution in both the high and low-gain regimes where the individual electron phase dependence is eliminated. Coupling to higher harmonics is also incorporated in the integral equation which is solved numerically on a small computer. The transverse optical mode remains fixed during this FEL interaction. However, fixed optical mode coupling is incorporated by including the filling factor.

b. Small-Signal Gain Formula

A modified small-signal gain formula, DAT, which incorporates harmonics and the broadening of the electron beam due to emittance and energy

spread was also used in developing the gain plots. Dattoli's parametrized gain formula [Ref. 20] is given in cgs units by

$$G = 19 \times 10^{-4} N^2 n^2 \cdot \frac{K^2}{1 + K^2} \cdot \frac{\hat{I}(A)}{\gamma} \cdot [J_{0,1}]^2 \cdot \frac{1}{(1 + \mu_c/3)(1 + (n\mu_x)^2)^2(1 + (n\mu_y)^2)(1 + 1.7(n\mu_e)^2)} \quad (69)$$

where

- G = single-pass gain,
- N = number of undulator periods,
- n = harmonic number,
- K = rms undulator parameter,
- $\hat{I}(A)$ = peak current in amperes,
- γ = Lorentz factor,
- $J_{0,1}$ = Bessel function = $[J(n-1)/2(n\xi) - J(n+1)/2(n\xi)]$ where $\xi = 1/2 K^2 / (1 + K^2)$,
- μ_c = coupling parameter,
- $\mu_{x,y}$ = broadening parameter due to emittance,
- μ_e = broadening parameter due to energy spread.

The parameterization of electron beam characteristics contained in (69) has been obtained by a polynomial expansion, and best fit with numerical data [Ref. 27,28]. The coupling parameter μ_c is inversely proportional to the rms longitudinal bunch length of the electron pulse and does not significantly contribute to degrading the gain since $\mu_c \ll 1$ for the cases considered. For an ideal linear undulator the magnetic field is constant along the x-direction. By ideal we mean undulator magnets that extend to infinity in the x-direction. In this case, electrons are not focused, but continue their motion away from the undulator-axis. For the ideal linear undulator the horizontal emittance can therefore be neglected, since it does not contribute to gain degradation. Dattoli's parametrized gain formula was modified by D. Warren to include these assumptions [private communication]. The modified small-signal gain formula (DAT) is written as

$$G = 19 \times 10^{-4} N^2 n^2 \cdot \frac{K^2}{1 + K^2} \frac{\hat{I}(A)}{\gamma} [J_{0,1}]^2 \cdot \frac{1}{1 + \left(2N_\beta \frac{e_y}{\gamma}\right)^2} \cdot \frac{1}{1 + 1.7(ES)^2} \quad (70)$$

where $ES = 2.8 n N (\Delta\gamma/\gamma)$
 e_y = rms emittance in y-direction
 N_β = number of Betatron oscillations.

This is peak gain at the optimum resonance condition.

A gain plot can be generated to illustrate the effects of emittance and energy spread for a given undulator and electron beam. This analysis, valid only in weak fields, is a one-dimensional theory where all transverse effects have been neglected. However, the size of the electron beam relative to the optical mode size is incorporated by including the filling factor. The five methods used are summarized below in Table II.

TABLE II.

	FEX	WFS	SIM	INT	DAT
high gain	yes	yes	yes	yes	no
mode distortion	yes	yes	no	no	no
energy spread	yes	no	yes	yes	yes
strong fields	yes	yes	yes	no	no
harmonics	yes	yes	yes	yes	yes

The high gain theories are non-linear in current j and are determined self-consistently. A theory with mode distortion describes a self-consistent calculation of the transverse optical wavefront without the use of the filling factor. Modeling the electron beam to include energy spread effects is

incorporated in all of the methods except WFS. The strong-field theories, FEX, WFS, and SIM are able to calculate gain in strong nonlinear fields. All methods of theoretical analysis include harmonic coupling using Bessel functions to express the reduced coupling. The gain for each theory is calculated with the optimum resonance condition.

These five methods each have their own merit in predicating gain. The FEX code incorporates as much physics as is feasible, but requires a CRAY computer and is not easy to use. The SIM, INT and 3-D WFS methods require only a personal computer, but do not include the full range effects in FEX. On the other hand, the parameterized gain formula, DAT, is valid only for small-signal gain in weak fields, but requires only a calculator for evaluation.

F. DISCUSSION OF THE PLOTS

Plots of gain for the three micro-undulators are shown in Figures 15 through 20. In Figure 15, gain is plotted against the rms energy spread for the undulator using the fundamental. The five methods of analysis, FEX, WFS, SIM, INT and DAT are shown. Only a single WFS data point is shown, indicated by an X, for a monoenergetic electron beam. The emittance is $\epsilon = \lambda/4$, and the filling factor found to be $\mathcal{F} = 0.25$. As expected, the gain decreases for all four methods, FEX, SIM, INT and DAT when the energy spread is increased to 0.3%. The characteristic energy spread, shown on the horizontal axis by an arrow, indicates where gain should be seriously degraded by the energy spread effect because the electron

GAIN VS ENERGY SPREAD

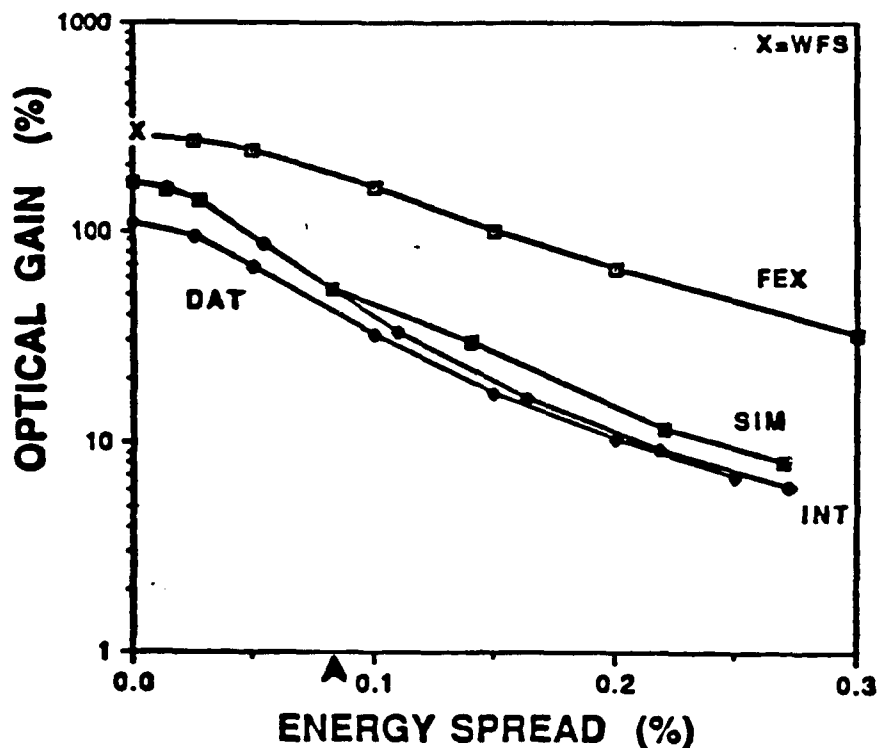


Figure 15. Gain Curve for Micro-undulator Design Operating on the Fundamental where Energy Spread is Varied.

phase is roughly equal to λ . FEX and WFS have nearly equal gain values, because they represent a complete self-consistent FEL oscillator solution where optical distortion of the optical wavefront is taken into account. The SIM and INT curves are below FEX for the entire energy spread range, because they do not include mode distortion. The DAT theory does not include mode distortion or self-consistent high gain, and therefore lies below all other theories.

Gain vs optical power for the fundamental undulator with nearly perfect electron beam quality, energy spread of 0% and $\epsilon = \lambda/4$, for FEX, SIM, and WFS are shown in Figure 16. The gain for the three methods starts to degrade at approximately the same optical power. The characteristic power where the beginning of saturation should occur is indicated by a star. The FEX and WFS curves are above the SIM curves, because mode distortion increases coupling at all powers. The 3-D codes agree throughout the entire power range except when the optical field becomes very strong. There, an exact calculation of gain from any FEL model becomes difficult.

Figure 17 displays gain vs energy spread for the second undulator design which operates on the third harmonic with design parameters given in Table I. The gain curve is similar to the previous design except that the filling factor is $\mathcal{F} = 0.1$. Similar trends in the gain degradation and saturation are seen in Figures 15 and 16, because of the attributes of the theoretical models used. However, this design, operates on the third harmonic with only $N=49$ periods compared to $N=413$ periods for the fundamental design. The sensitivity of gain to energy spread is reduced significantly as shown in Figures 15 and 16. The gain vs optical power plot, shown in Figure 18, illustrates the additional advantage of using harmonics since the characteristic power for saturation $6 \times 10^9 \text{ W/cm}^2$, is approximately a factor of 15 higher than in the fundamental design. As seen in Figure 18 some

GAIN VS POWER

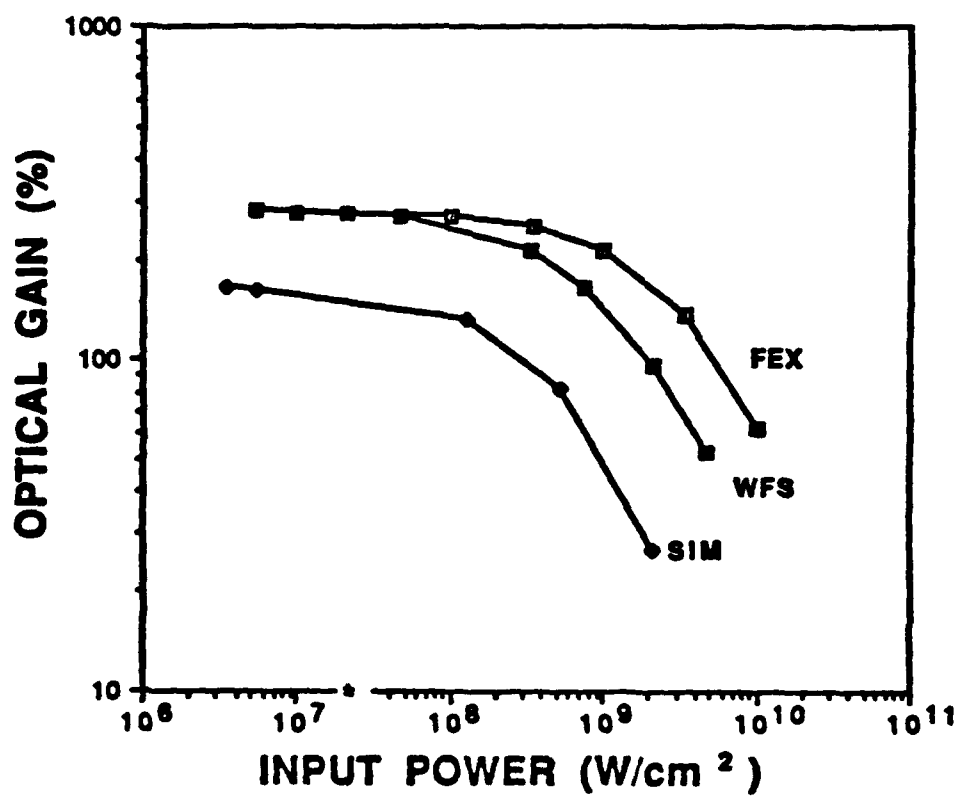


Figure 16. Gain Curve for Micro-undulator Design Operating on the Fundamental where Optical Power is Varied.

GAIN VS ENERGY SPREAD

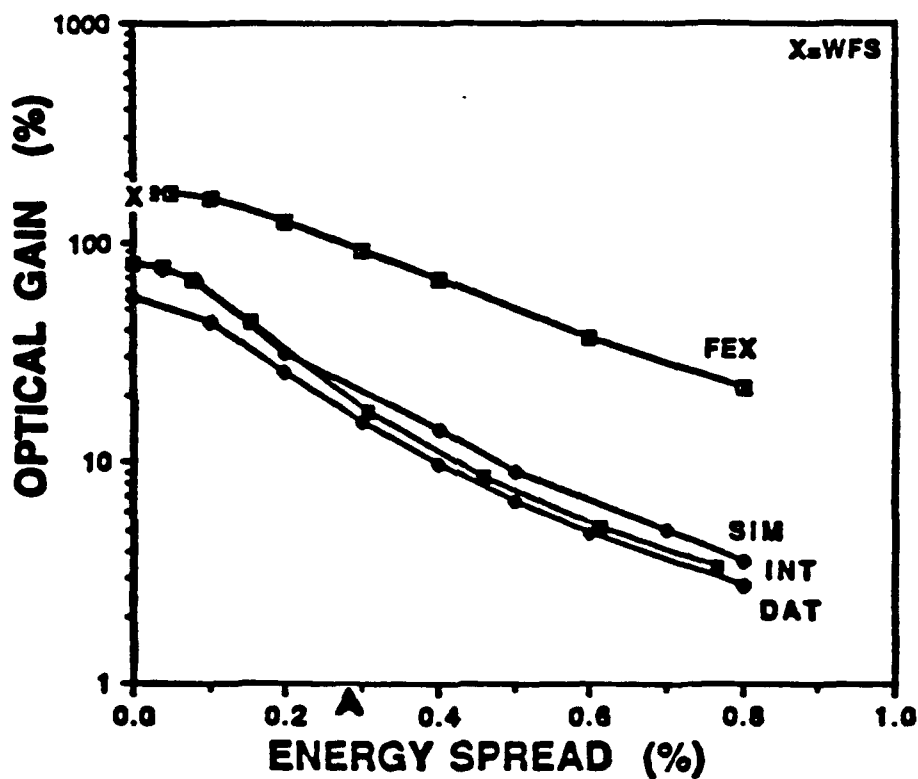


Figure 17. Gain Curve for Micro-undulator Design Operating on the Third Harmonic where Energy Spread is Varied.

GAIN VS POWER

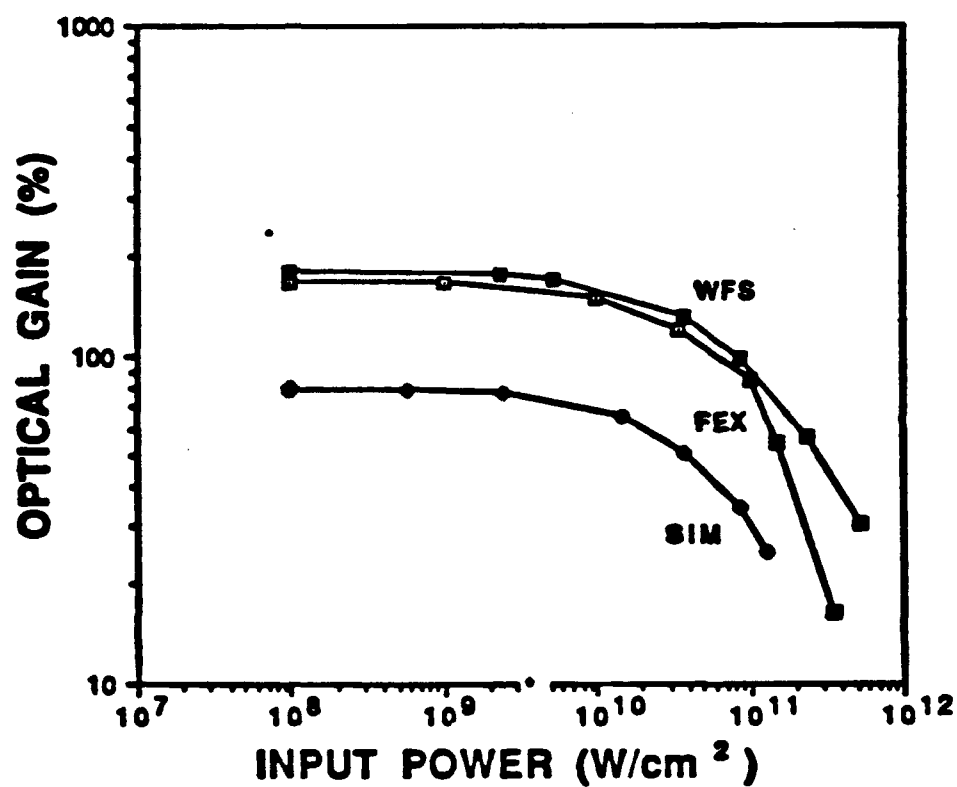


Figure 18. Gain Curve for Micro-undulator Design Operating on the Third Harmonic where Optical Power is Varied.

deviations between FEX and WFS occur at very high powers where calculations are difficult.

Extending the comparison to the third undulator operating in the ninth harmonic, Figure 19 shows the same general features as in the previous gain vs energy spread plots. Only $N=19$ periods are required here compared to $N=49$ periods for the third harmonic design and $N=413$ in the fundamental design. The gain vs optical power plot, Figure 20, illustrates the same shape for the three methods as the third harmonic design. However, the characteristic power for saturation $7 \times 10^9 \text{ W/cm}^2$ is approximately a factor of 20 higher than found in the fundamental design.

GAIN VS ENERGY SPREAD

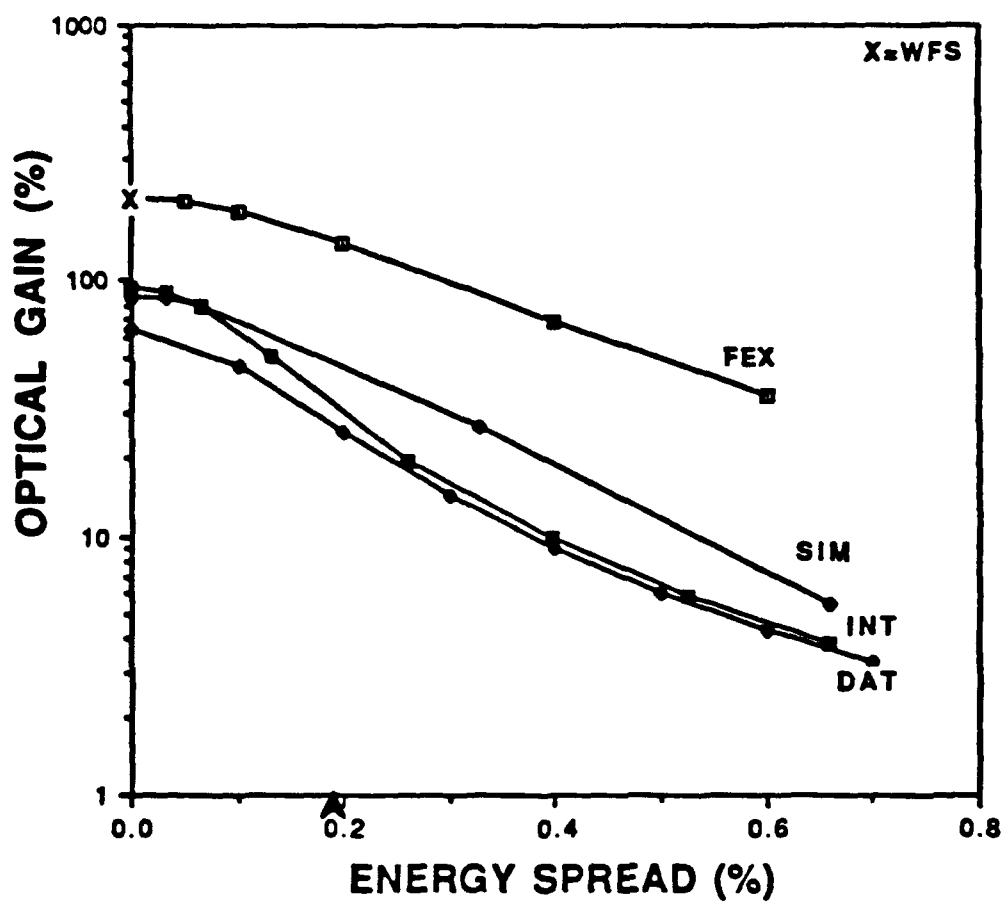


Figure 19. Gain Curve for Micro-undulator Design Operating on the Ninth Harmonic where Energy Spread is Varied.

GAIN VS POWER

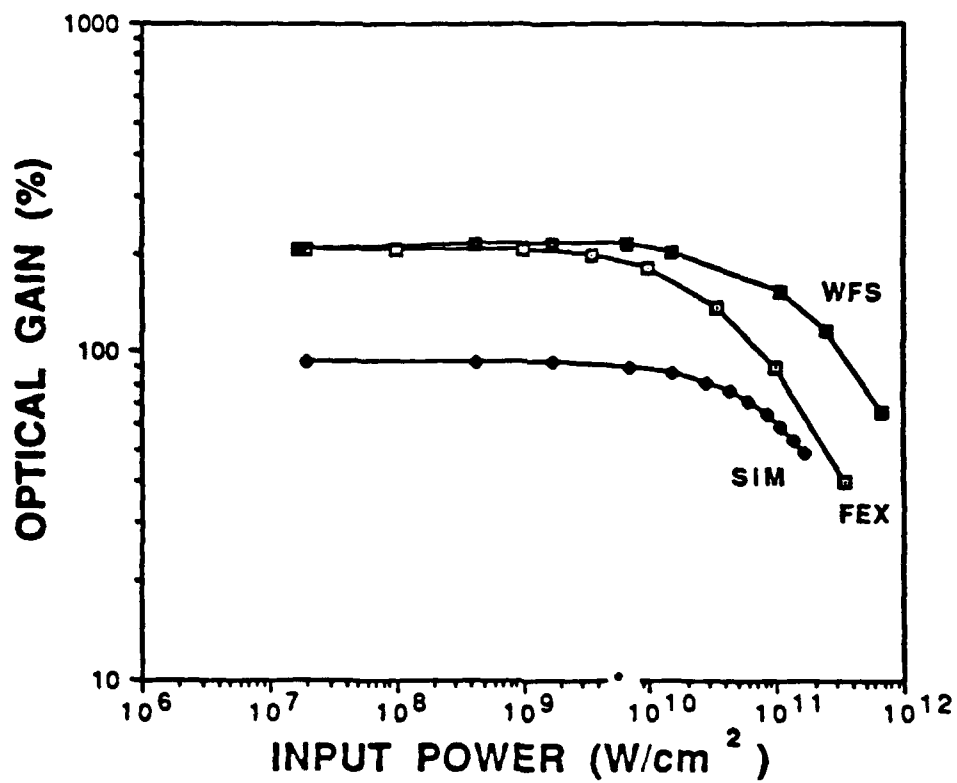


Figure 20. Gain Curve for Micro-undulator Design Operating on the Ninth Harmonic where Optical Power is Varied.

V. CONCLUSIONS

Preliminary designs of Compact Free Electron Lasers are analyzed. This work contributes to the operational advancement of Compact FELs by illustrating the advantages of using harmonics where size and complexity would be substantially reduced. The device would be available to a wider range of users with many potential applications in scientific and modern technology. Three micro-undulator designs are explored to reach an optical wavelength of 0.4 microns with an electron beam of 20 Mev. The use of harmonics at short wavelengths improves the undulator design with longer periods that would be easier to fabricate. The use of shorter undulators *minimizes the penalty from emittance and energy spread* inherent in all electron beams. For fixed optical wavelength, and an undulator using harmonics, the electron beam energy can be reduced thereby lowering the radiation shielding requirements for personnel. Operation over a wider range of wavelengths and the increase in optical power available at saturation provide additional benefits of using harmonics. The value of using harmonics to improve undulator designs are evident by performance calculations conducted by various computer codes, and should be pursued to extend this new scientific tool for future applications.

LIST OF REFERENCES

- [1] Madey, J. M. J., *J. Applied Physics* **42**, 1906 (1971).
- [2] Colson, W. B., A. M. Sessler, "Free Electron Lasers," *Annual Review Particle Science*, **35**, 25 (1985).
- [3] Colson, W. B., S. K. Ride, "The Free Electron Laser: Maxwell's Equations Driven by Single Particle Currents," *Physics of Quantum Electronics*, **7**, 377 (1980).
- [4] Colson, W. B., "Tutorial on Classical Free Electron Laser Theory," *Nuclear Instruments and Methods*, **A237**, 1 (1985).
- [5] Colson, W. B., C. Pellegrini and A. Reneiri, "Classical Free Electron Laser Theory," *Free Electron Laser Handbook*, **Ch. 5** North-Holland Handbook Series, 115 (1990).
- [6] Colson, W. B., "The Nonlinear Wave Equation for Higher Harmonics in Free-Electron Lasers," *IEEE Journal of Quantum Electronics*, **QE-17**, No. 8, 1417 (1981).
- [7] Schmitt, M. J., "Harmonic Production in Free-Electron Lasers," Ph.D. Thesis, UCLA, (1987).
- [8] Goldstein, J. C., Sheffield, R. L., Carlsten B. E., Warren R. W., "Compact RF-Linac Free-Electron Lasers," *Nuclear Instruments and Methods in Physics Research*, **A28**, 1 (1989).
- [9] Goldstein, J. C., Newnam, B. E., Cooper, R. K., and Comly, Jr., "An XUV/VUV Free-Electron Laser Oscillator," *American Institute of Physics*, **No.118**, 293 (1984).
- [10] Jackson, J. D., *Classical Electrodynamics*, John Wily & Sons, Inc., New York-London, (1962).
- [11] Colson, W. B., "Free Electron Laser Theory," Ph.D. Thesis, Stanford University, (1977).

- [12] Colson, W. B., " Free-Electron Lasers Operating in Higher Harmonics," *The American Physical Society, Physical Review A*, **24**, No. 1, 639 (1981).
- [13] Sheffield, R. L., " High-Brightness Electron Injectors: A Review," to be published in the 1989 Particle Accelerator Conference Proceedings, Chicago, IL, March, (1989).
- [14] Sheffield, R. L., " High-Brightness Injectors for RF-Driven Free-Electron Lasers," *IEEE Journal of Quantum Electronics*, **QE-23**, No.9, 1489 (1987).
- [15] LeJune, C. and Aubert, J., " Emittance and Brightness: Definitions and Measurements, Applied Charge Particle Optics," A. Septier, ED., *Advances in Electronics and Electron Physics*, **Supp, 13A**, 768 (1980).
- [16] Warren, R. W., Feldman, D. W., Preston, D., " High-Field Pulsed Microwigglers," to be published in *Nuclear Instruments and Methods in Physics Research*, **AXX,xx** (1990).
- [17] Sheffield, R. L., private communication.
- [18] Warren, R. W., " Lasing on Higher Harmonics," to be published in *Nuclear Instruments and Methods in Physics Research*, **AXX,xx** (1991).
- [19] Goldstein, J. C., McVey, B. D., Tokar, R. L., Elliott, C. J., Schmitt, M. J., Carlsten, B. E., Thode, L. E., " Simulation Codes for Modeling Free-Electron Laser Oscillators," to be published in the 1990 Proceedings ~~SE~~ 1045, Modeling and Simulation of Laser Systems, Los Angeles, CA, January, (1989).
- [20] Dattoli, G., Letardi, T., Madey, J. M. J., and Renieri, A., " Limits on the Single-pass Higher Harmonics FEL Operation," *IEEE Journal of Quantum Electronics*, **QE-20**, No. 9, 1003 (1984).
- [21] Park, S. Y., Baird, J. M., Smith, R. A., and Hirshfield, J. L., " Exact Magnet Field of a Helical Wiggler," *Applied Physics*, **53(3)**, 1320 (1982).
- [22] Colson, W. B., Blau, J., " Free-Electron Laser Theory in Weak Optical Fields," to be published in *Nuclear Instruments and Methods in Physics Research*, **A272**, 386 (1989).
- [23] Colson, W. B., Gallardo J. C., Bosco P. M., " Free-Electron Laser Gain Degradation and Electron Beam Quality," *Physical Review A*, **34**, 4875 (1986).

- [24] Kogelnik, H., Li, T., "Laser Beams and Resonators," *Proceedings of the IEEE*, **54**, No. 10, 1312 (1966).
- [25] McVey, B. D., "Three-dimensional Simulations of Free-Electron Laser Physics," *Nuclear Instruments and Methods in Physics Research*, **A250**, 449 (1986).
- [26] McVey, B. D., Goldstein, J. C., Tokar, R. L., Elliott, C. J., Gitomer, S. J., Schmitt, M. J., Thode, L. E., "Numerical Simulations of Free-Electron Laser Oscillators," to be published in *Nuclear Instruments and Methods in Physics Research*, **A285**, 186 (1989).
- [27] Dattoli, G., Letardi, T., Madey, J. M. J., and Renieri, A., "Lawson-Penner Limit and Single Passage Free-Electron Lasers Performances," *IEEE Journal of Quantum Electronics*, **QE-20**, No. 6, 637 (1984).
- [28] Ciocci, F., Dattoli, G., Renieri, A., "Comments on the Gain Calculation of a FEL Operating with a Linearly Polarized Wiggler," *Nuovo Cimento Letter*, **34**, 341 (1982).

INITIAL DISTRIBUTION LIST

- | | | |
|----|---|---|
| 1. | Defence Technical Information
Cameron Station
Alexandria, Virginia 22304-6145 | 2 |
| 2. | Library Code 52
Naval Post Graduate School
Monterey, California 93943-5002 | 2 |
| 3. | Department Chairman, Code PH
Department of Physics
Naval Post Graduate School
Monterey, California 93943-5002 | 1 |
| 4. | Professor W. B. Colson Code PH/Cw
Department of Physics
Naval Post Graduate School
Monterey, California 93943-5002 | 4 |
| 5. | Dr. Roger W. Warren
Los Alamos National Laboratory
M/S 817
P.O. Box 1663
Los Alamos, New Mexico 87545 | 1 |
| 6. | Randy Souza
188 Hathaway Street
New Bedford, Massachusetts 02746 | 4 |